

---

# Transition Path Sampling Methods

C. Dellago<sup>1</sup>, P.G. Bolhuis<sup>2</sup>, and P.L. Geissler<sup>3</sup>

<sup>1</sup> Faculty of Physics, University of Vienna, Boltzmanngasse 5, 1090 Wien, Austria  
[Christoph.Dellago@univie.ac.at](mailto:Christoph.Dellago@univie.ac.at)

<sup>2</sup> van 't Hoff Institute for Molecular Sciences, University of Amsterdam, Nieuwe Achtergracht 166, 1018 WV Amsterdam, The Netherlands  
[bolhuis@science.uva.nl](mailto:bolhuis@science.uva.nl)

<sup>3</sup> Department of Chemistry, University of California at Berkeley, 94720 Berkeley, CA, USA  
[geissler@cchem.berkeley.edu](mailto:geissler@cchem.berkeley.edu)



Christoph Dellago

<b>1</b>	<b>Introduction</b>	351
<b>2</b>	<b>The Transition Path Ensemble</b>	353
2.1	Path Probability	354
2.2	Reactive Pathways	355
2.3	Path Probabilities for Deterministic and Stochastic Dynamics	356
2.4	Defining the Stable States $A$ and $B$	358
<b>3</b>	<b>Sampling Path Ensembles</b>	359
3.1	Monte Carlo in Path Space	359
3.2	Shooting and Shifting	361
3.3	Generating an Initial Path	365
<b>4</b>	<b>Reaction Mechanisms: Analyzing Transition Pathways</b>	366
4.1	Reaction Coordinate vs. Order Parameter	367
4.2	Committor	368
4.3	The Transition State Ensemble	369
4.4	Committor Distributions	370
<b>5</b>	<b>Kinetics</b>	372
5.1	Reaction Rate Constants and Population Fluctuations	373
5.2	Free Energies in Path Space	376
5.3	Umbrella Sampling	377
5.4	Reversible Work to Change the Path Length	378
5.5	Transition Interface Sampling and Partial Path Sampling	380
5.6	Calculating Activation Energies with Transition Path Sampling	383
<b>6</b>	<b>Rare Events in Trajectory Space</b>	383
<b>References</b>		389

Transition path sampling, based on a statistical mechanics in trajectory space, is a set of computational methods for the simulation of rare events in complex systems. In this chapter we give an overview of these techniques and describe their statistical mechanical basis as well as their application.

## 1 Introduction

This chapter will be focused on computer simulation algorithms to overcome the problem of widely disparate time scales. In doing that we concentrate on processes dominated by rare events: events that occur only rarely, but when they occur, they occur quickly. Examples of such processes include the nucleation of first order phase transitions, chemical reactions in solution and on surfaces, transport in and on solids, and protein folding to name but a few. The occurrence of rare events is related to *high potential energy barriers* or *entropic bottlenecks* (narrow but energetically flat passageways in configuration space [1]) partitioning the configuration space of the system into (meta)stable basins. In equilibrium, the system spends the bulk of its time fluctuating within these long-lived stable states and barriers are crossed only very rarely. In order to understand such processes in detail it is necessary to identify the relevant degrees of freedom and to separate them from orthogonal variables which may be regarded as random noise. While in principle conventional computer simulations can provide the information necessary to do that, the wide gap in time scales originating in the long times between barrier crossings is a serious computational problem.

The straightforward approach to this kind of difficulty is to follow the time evolution of the system, for instance by molecular dynamics simulation, and wait until a sufficient number of events have been observed. However, the computational requirements of such a procedure are excessive for most interesting systems. In practice, it is frequently impossible to observe a single transition of interest, let alone collect enough statistics for a microscopic resolution of the mechanism. For instance, reaction times of chemical reactions occurring in solution often exceed the second time scale. Since the simulation of molecular systems typically proceeds in steps of roughly one femtosecond, of the order of  $10^{15}$  steps are required to observe just one transition. Such calculations are far beyond the reach of the fastest computers even in the foreseeable future.

A different strategy to approach such problems is to search for the dynamical bottlenecks through which the system passes during a transition between metastable states. If the dynamics of the system is dominated by energetic effects (as opposed to entropic effects), such bottlenecks can be identified with saddle points in the potential energy surface. In this case, saddle points are transition states, activated states from which the system can access different stable states through small fluctuations. Comparing stable states with transition states one can often infer the mechanism of the reaction. Reaction rate constants, which are very important because they are directly comparable to

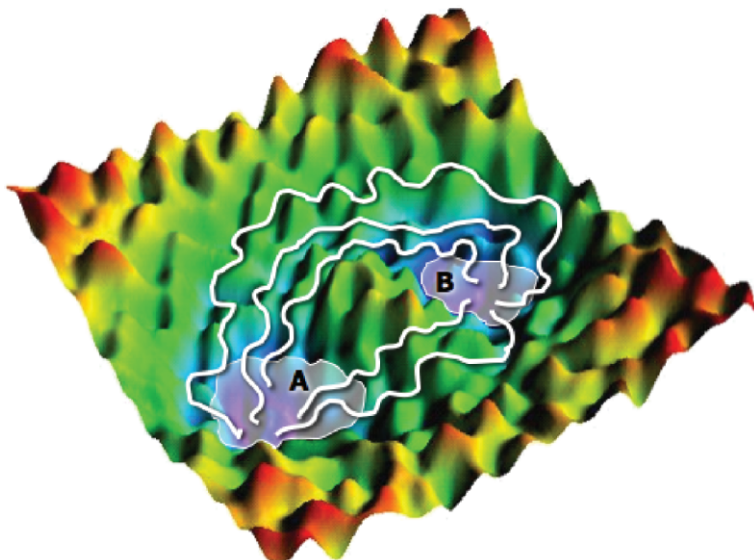


**Fig. 1.** Transitions pathways connecting stable states *A* and *B* on a caricature of a complex energy landscape

experimental observables, can then be determined via transition state theory (TST). If the transition state theory estimate of the reaction rate constant is not sufficiently accurate, the reactive flux formalism, in which dynamical corrections to simple transition state theory are calculated from dynamical trajectories initiated at the transition state, can provide the desired corrections [2].

While transition state theory and its modern variants can be very successful in simple (small or highly ordered) systems, complex systems with strongly non-linear potential energy landscapes require an entirely different approach. In such complex systems the saddle points in the potential energy surface cease to be characteristic points of the free energy barrier. Instead, the free energy barrier may encompass a large set of configurations some of which are stationary points but most are not (see Fig. 1). One may hope to be guided by physical intuition in the search of transition states, in effect postulating the reaction coordinate. But the relevant degrees of freedom may be highly collective and therefore difficult to anticipate. This problem can be overcome with the transition path sampling approach [3–6]. Based on a statistical mechanics of trajectories, this method focuses on those segments of the time evolution where the rare, but important events actually occur, thus avoiding long intervening waiting times between. Since in such a complex system rare transitions between stable states can occur via a multitude of different pathways, the notion of a single, well-defined reaction path, such as a zero kinetic energy path, is abandoned in favor of a large set of possibly

markedly different paths: the *transition path ensemble*. Defining this ensemble does not require any a priori knowledge on how the process occurs, i.e., no definition of a reaction coordinate is necessary. Instead, it is sufficient to specify unambiguously the initial and the final state of the transition. This is a crucial feature of the method since information on the reaction coordinate is usually unavailable. Transition path sampling can therefore be used to study rare transitions between long-lived stable states in complex systems characterized by a rugged potential energy surface. Other path based methods that can be used to study rare events include the so called string method [7, 8] applicable to stochastic dynamics and methods based on the minimization of the classical action [9, 10]. Both of these approaches will be discussed in detail in other contributions to this summer school.

The transition path sampling techniques developed for the study of rare events can also be used to improve the calculation of free energies from non-equilibrium transformations on the basis of Jarzynski's theorem. In this approach equilibrium free energies are linked to the statistics of work performed during irreversible transformations. When applying these ideas in computer simulations, one has to deal with rare events (of a different kind, however) and transition path sampling can help to solve this problem. Due to space limitations we cannot comprehensively discuss all aspects of transition path sampling in this chapter. For further information the reader is referred to several recent review articles [11–15]. Of these articles, [12] is the most detailed and comprehensive.

## 2 The Transition Path Ensemble

Figure 1 depicts the general situation that can be addressed with the transition path sampling methodology:

- The system is (meta)stable in states  $A$  and  $B$  in the sense that if the system is put there it will remain there for a long time. We assume that states  $A$  and  $B$  can be easily characterized using an order parameter.
- The system evolves according to deterministic or stochastic equations of motion.
- The system spends most of its time either in  $A$  or  $B$  but, rarely, transition between the stable states  $A$  and  $B$  occur.
- No long-lived metastable states exist between states  $A$  and  $B$ .
- The stable states are separated by an unknown and, in general, rough energy or free energy barrier.

The goal of a transition path sampling simulation is to collect all likely transition pathways. These pathways can then be analyzed to find the transition mechanism, i.e., to identify the degrees of freedom that capture the physics of the transition and to determine how they change during the transition. Since

the pathways collected with transition path sampling are fully dynamical trajectories rather than artificial pathways such as minimum energy pathways or elastic bands, it is also possible to extract kinetic information from transition path sampling simulations. The first step in the application of transition path sampling consists in the definition of an appropriate path ensemble. This is what we will do next.

## 2.1 Path Probability

It is convenient to discretize the continuous time evolution of the system and view a trajectory of length  $T$  as an ordered sequence of states:

$$x(\mathcal{T}) \equiv \{x_0, x_{\Delta t}, x_{2\Delta t}, \dots, x_T\}. \quad (1)$$

Consecutive states are separated by a small time increment  $\Delta t$  and  $x_{i\Delta t}$  is a complete snapshot of the system at time  $i\Delta t$ . For a molecular system evolving according to Newton's equations of motion, for instance,  $x$  comprises the positions  $r$  and momenta  $p$  of all particles. Since the trajectory  $x(\mathcal{T})$  results from slicing the continuous path in time, the states  $x_{i\Delta t}$  are often called *time slices* (see Fig. 2).

The probability (density) to observe a given path  $x(\mathcal{T})$  depends on the probability of its initial condition and the specific dynamics of the system. For Markovian processes, i.e., processes for which the probability to move from  $x_t$  to  $x_{t+\Delta t}$  after one time step  $\Delta t$  depends only on  $x_t$  and not on the history of the system prior to  $t$ , the total path probability can be written as the product of single time step transition probabilities  $p(x_t \rightarrow x_{t+\Delta t})$ ,

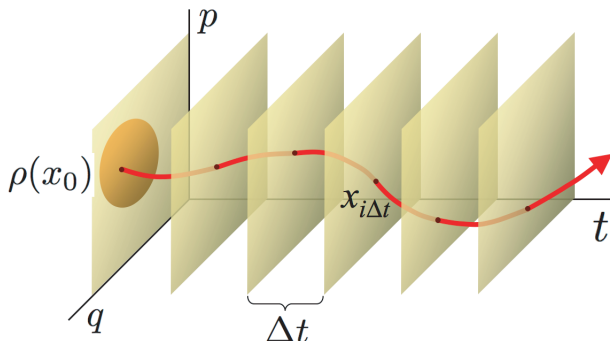


**Fig. 2.** A trajectory is discretized into “time slices” separated by a time increment  $\Delta t$ . Time slice  $x_{i\Delta t}$  is a complete description of the system at time  $i\Delta t$ . For Newtonian and Langevin dynamics each time slice consists of the positions and momenta of all particles. Initial conditions for the trajectories are distributed according to  $\rho(x_0)$

$$\mathcal{P}[x(\mathcal{T})] = \rho(x_0) \prod_{i=0}^{\mathcal{T}/\Delta t - 1} p(x_{i\Delta t} \rightarrow x_{(i+1)\Delta t}) . \quad (2)$$

The first factor on the right hand side of the above equation,  $\rho(x_0)$ , is the probability distribution of the initial conditions. The particular form of the transition probability  $p(x_t \rightarrow x_{t+\Delta t})$  for different types of deterministic and stochastic dynamics will be discussed below.

## 2.2 Reactive Pathways

Since we want to focus on reactive pathways we now restrict the path ensemble to those pathways that start in region  $A$ , the *reactant* region, and end in region  $B$ , the *product* region. This is achieved by multiplying the path probability  $\mathcal{P}[x(\mathcal{T})]$  with the appropriate characteristic functions:

$$\mathcal{P}_{AB}[x(\mathcal{T})] \equiv h_A(x_0) \mathcal{P}[x(\mathcal{T})] h_B(x_{\mathcal{T}}) / Z_{AB}(\mathcal{T}) . \quad (3)$$

Here,  $h_A(x)$  is the characteristic function of region  $A$  which is unity if the argument  $x$  is inside  $A$  and vanishes otherwise, and  $h_B(x)$  is defined similarly:

$$h_{A,B}(x) = \begin{cases} 1 & \text{if } x \in A, B \\ 0 & \text{if } x \notin A, B \end{cases} . \quad (4)$$

Due to the restriction applied to the pathways in the transition path probability (3) a path not beginning in  $A$  or not ending in  $B$  (or both) has a statistical weight of zero. A path connecting  $A$  and  $B$ , on the other hand, may have a non-zero weight that depends on the unrestricted path probability  $\mathcal{P}[x(\mathcal{T})]$ . The transition path ensemble (3) selects only the reactive trajectories from the ensemble of all possible pathways while leaving the relative probabilities of the reactive trajectories among each other unchanged. Since by multiplication with the characteristic functions we have reduced the size of the path ensemble, the probability distribution is normalized by

$$Z_{AB}(\mathcal{T}) \equiv \int \mathcal{D}x(\mathcal{T}) h_A(x_0) \mathcal{P}[x(\mathcal{T})] h_B(x_{\mathcal{T}}) . \quad (5)$$

The notation  $\int \mathcal{D}x(\mathcal{T})$ , familiar from path integral theory, implies a summation over all pathways:

$$\int \mathcal{D}x(\mathcal{T}) \equiv \int \cdots \int dx_0 dx_{\Delta t} dx_{2\Delta t} \cdots dx_{\mathcal{T}} . \quad (6)$$

The transition path ensemble (3) is a complete statistical description of all possible pathways connecting reactants with products. Pathways sampled according to this ensemble are typical trajectories which can then be analyzed to yield information about mechanisms and rates. The definition of the transition path ensemble is very general and valid for all Markovian processes. In the following we will write down the specific form of the transition path ensemble for different types of processes.

### 2.3 Path Probabilities for Deterministic and Stochastic Dynamics

The general transition path sampling formalism can be applied to various ensembles of pathways differing both in the distributions of initial conditions as well as in the particular transitions probabilities. The specific form of the path probability depends on the process one wants to study and is not imposed by the transition path sampling technique itself. In the following we discuss several path probabilities that frequently occur in the study of condensed matter systems.

#### Initial Conditions

If initial conditions are prepared by placing the system in contact with a heat bath at a specific temperature  $T$  the distribution of initial conditions is the *canonical* one,

$$\rho(x) = \exp\{-\beta\mathcal{H}(x)\}/Z, \quad (7)$$

where

$$Z(\beta) = \int dx \exp\{-\beta\mathcal{H}(x)\} \quad (8)$$

is the partition function of the system,  $\mathcal{H}(x)$  is its Hamiltonian, and  $\beta = 1/k_B T$  is the inverse temperature. In other situations the energy  $E$  of the initial states is well defined requiring the use of the *microcanonical* distribution,

$$\rho(x) = \delta[E - \mathcal{H}(x)]/g(E), \quad (9)$$

where

$$g(E) = \int dx \delta[E - \mathcal{H}(x)] \quad (10)$$

is the density of states. Different distributions of initial conditions can easily be incorporated into the path sampling scheme as well. Indeed, path sampling can be applied even in the case on non-equilibrium systems where the distribution of initial conditions is not known explicitly [16].

#### Newtonian Dynamics

Consider a classical molecular system that evolves according to Hamilton's equations of motion,

$$\dot{r} = \frac{\partial \mathcal{H}(r, p)}{\partial p}, \quad \dot{p} = -\frac{\partial \mathcal{H}(r, p)}{\partial r}. \quad (11)$$

Since the time evolution of such a system is deterministic, the state of the system  $x_t$  at time  $t$  is completely determined by the state  $x_0$  at time 0:

$$x_t = \phi_t(x_0). \quad (12)$$

Here,  $x = \{r, p\}$  includes the positions  $r$  and momenta  $p$  of all particles. The time dependent function  $\phi_t(x_0)$  is the *propagator* of the system. For such deterministic dynamics the short time transition probability can be written in terms of a Dirac delta function:

$$p(x_t \rightarrow x_{t+\Delta t}) = \delta[x_{t+\Delta t} - \phi_{\Delta t}(x_t)] . \quad (13)$$

Accordingly, the path probability is given by

$$\mathcal{P}_{AB}[x(\mathcal{T})] = \rho(x_0)h_A(x_0) \prod_{i=0}^{\mathcal{T}/\Delta t - 1} \delta[x_{(i+1)\Delta t} - \phi_{\Delta t}(x_{i\Delta t})]h_B(x_{\mathcal{T}})/Z_{AB}(\mathcal{T}) , \quad (14)$$

where the partition function

$$Z_{AB}(\mathcal{T}) = \int dx_0 \rho(x_0)h_A(x_0)h_B(x_{\mathcal{T}}) , \quad (15)$$

normalizes the distribution. Here, all but the first state of the pathway,  $x_0$ , have been integrated out and the remaining integral is over initial conditions only. Other examples of deterministic dynamics include the extended Lagrangian dynamics of Car and Parrinello [17] and various dynamics with thermostats such as the Nose-Hoover thermostat [18] or the Gaussian isokinetic thermostat [19]. Also for these types of dynamics the above definition of the transition path ensemble applies.

## Brownian Dynamics

As an example for a stochastic process consider a system evolving according to the Langevin equation in the high friction limit where inertial effects can be neglected and momenta are not required for the description of the system:

$$m\gamma\dot{r} = -\frac{\partial V(r)}{\partial r} + \mathcal{F} . \quad (16)$$

Here,  $m$  is the mass of the particles,  $V(r)$  the potential energy of the system,  $\gamma$  the friction constant, and  $\mathcal{F}$  is a Gaussian random force uncorrelated in time that satisfies the fluctuation dissipation theorem [20]

$$\langle \mathcal{F}(t)\mathcal{F}(0) \rangle = 2m\gamma k_B T\delta(t) . \quad (17)$$

Due to the random force the time evolution of the system in a short time step  $\Delta t$  consists of a systematic part depending on the force  $-\partial V/\partial r$  and a random displacement  $\delta r$  [21, 22]:

$$r_{t+\Delta t} = r_t - \frac{\Delta t}{\gamma m} \frac{\partial V}{\partial r} + \delta r . \quad (18)$$

This random displacement is a Gaussian random variable with zero mean and a width  $\sigma$  that depends on the time step and the temperature [21, 22],

$$\sigma^2 = \frac{2k_{\text{B}}T}{m\gamma} \Delta t. \quad (19)$$

The short time transition probability then follows from the statistics of the random displacement:

$$p(r_t \rightarrow r_{t+\Delta t}) = \frac{1}{\sqrt{2\pi\sigma^2}} \exp \left\{ -\frac{(r_{t+\Delta t} - r_t + \frac{\Delta t}{\gamma m} \frac{\partial V}{\partial r})^2}{2\sigma^2} \right\}. \quad (20)$$

Appropriate expressions for the short time transition probability  $p(x_t \rightarrow x_{t+\Delta t})$  can be derived also for Langevin dynamics with arbitrary friction and for Monte Carlo “dynamics” [4, 12].

## 2.4 Defining the Stable States $A$ and $B$

While a transition path sampling simulation does not require knowledge of a *reaction coordinate* capable of characterizing the progress of a transition through the dynamical bottleneck region, a careful definition of the initial region  $A$  and the final region  $B$  is important. Regions  $A$  and  $B$  are most conveniently characterized by the value of a low dimensional *order parameter*  $q$ . Often, defining a good order parameter capable of discriminating between  $A$  and  $B$  is far from trivial. For example, to define stable states for autoionization in liquid water the connectivity of the hydrogen bond network has to be taken into account [23].

The definitions of stable states  $A$  and  $B$ , and hence of the order parameter  $q$ , have to meet several criteria. First,  $A$  and  $B$  have to be large enough to accommodate typical equilibrium fluctuations. If this is not the case important transition pathways might be missing from the transition path ensemble. Second, region  $A$  spanned by  $h_A(x)$  and region  $B$  spanned by  $h_B(x)$  should be located entirely within the corresponding basins of attraction. In other words, region  $A$  should not overlap with the basin of attraction of  $B$  and vice versa. The basin of attraction of a specific stable state consists of all configurations from which trajectories relax into that stable state. If this second criterion is not met, the transition path sampling algorithm most likely collects non-reactive trajectory.

Correct definition of regions  $A$  and  $B$  may require considerable trial and error experimentation. Fortunately, it is easy to detect problems associated with an inappropriate choice of order parameter. For instance, short trajectories initiated from the initial point of the unsuccessful trajectory in Fig. 3 (solid line) will most likely end with a value of  $q$  characteristic of the final state. In contrast, the probability to relax into  $B$  from the initial point of the dashed trajectory is negligible. When problems are caused by non-discriminating regions  $A$  and  $B$ , the order parameter has to be refined until correct sampling can be achieved.

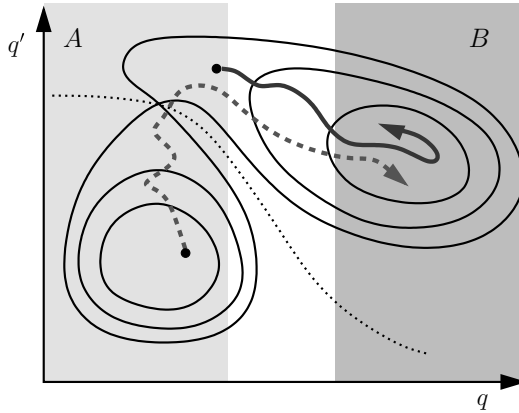


**Fig. 3.** In this free energy landscape the coordinate  $q$  fails to distinguish the basins of attraction of the stable states. If region  $A$  is defined by requiring that  $q$  is less than some limit (light gray region), points belonging to the basin of attraction of  $B$  are located inside  $A$ . Path starting from such points (such as the dark gray path) belong to the path ensemble but are not real reactive trajectories. For a correct definition of the stable states also the variable  $q'$  must be taken into account

### 3 Sampling Path Ensembles

Various deterministic and stochastic sampling techniques for path ensembles have been proposed [4–6]. Here we consider only Monte Carlo methods. It is important, however, to be aware that while the path ensemble is sampled with a Monte Carlo procedure each single pathway is a fully dynamical trajectory such as one generated by molecular dynamics.

#### 3.1 Monte Carlo in Path Space

In a transition path sampling simulation the goal is to collect reactive trajectories according to their weight in the transition path ensemble. This can be achieved with a Monte Carlo importance sampling procedure similar to a Monte Carlo simulation of, say, an atomic fluid. In the latter case, configurations are sampled by iterating a basic step: first a new configuration is generated from an old one by, for instance, displacing a randomly selected particle by a random amount. Then, the new configuration is accepted or rejected according to how the probability of the new configuration has changed with respect to the probability of the old configuration. Usually, the Metropolis rule is used to obtain an acceptance probability that satisfies the detailed balance condition. Provided that the algorithm is ergodic (i.e. that any configuration can be reached from any other configuration in a finite number of steps), this choice guarantees that the desired distribution of configurations

is sampled. Since this procedure generates a random walk that visits configurations according to their statistical weight, it is also called *importance sampling*.

Monte Carlo procedures can be applied very generally to sample probability distributions [24]. In particular, Monte Carlo techniques can also be used to sample ensembles of pathways. In this case a random walk is carried out in the space of trajectories instead of configuration space. The basic step of this procedure consists of generating a new path,  $x^{(n)}(\mathcal{T})$ , from an old one,  $x^{(o)}(\mathcal{T})$ . To guarantee that pathways are visited with a frequency proportional to their weight in the path ensemble  $\mathcal{P}_{AB}[x(\mathcal{T})]$  we require that the forward move from the old path to the new one must be exactly balanced by the reverse move:

$$\begin{aligned} \mathcal{P}_{AB}[x^{(o)}(\mathcal{T})] \pi[x^{(o)}(\mathcal{T}) \rightarrow x^{(n)}(\mathcal{T})] \\ = \mathcal{P}_{AB}[x^{(n)}(\mathcal{T})] \pi[x^{(n)}(\mathcal{T}) \rightarrow x^{(o)}(\mathcal{T})]. \end{aligned} \quad (21)$$

In this *detailed balance* condition  $\pi[x^{(o)}(\mathcal{T}) \rightarrow x^{(n)}(\mathcal{T})]$  is the probability to move from the old to the new path. According to the Monte Carlo generation and acceptance/rejection scheme, this probability is the product of a generation probability  $P_{\text{gen}}$  and an acceptance probability  $P_{\text{acc}}$ :

$$\begin{aligned} \pi[x^{(o)}(\mathcal{T}) \rightarrow x^{(n)}(\mathcal{T})] \\ = P_{\text{gen}}[x^{(o)}(\mathcal{T}) \rightarrow x^{(n)}(\mathcal{T})] \times P_{\text{acc}}[x^{(o)}(\mathcal{T}) \rightarrow x^{(n)}(\mathcal{T})]. \end{aligned} \quad (22)$$

From the detailed balance criterion (21) one obtains the following condition that must be obeyed by the acceptance probability:

$$\frac{P_{\text{acc}}[x^{(o)}(\mathcal{T}) \rightarrow x^{(n)}(\mathcal{T})]}{P_{\text{acc}}[x^{(n)}(\mathcal{T}) \rightarrow x^{(o)}(\mathcal{T})]} = \frac{\mathcal{P}_{AB}[x^{(n)}(\mathcal{T})] P_{\text{gen}}[x^{(n)}(\mathcal{T}) \rightarrow x^{(o)}(\mathcal{T})]}{\mathcal{P}_{AB}[x^{(o)}(\mathcal{T})] P_{\text{gen}}[x^{(o)}(\mathcal{T}) \rightarrow x^{(n)}(\mathcal{T})]}. \quad (23)$$

This relation can be satisfied by the Metropolis rule [25]

$$P_{\text{acc}}[x^{(o)}(\mathcal{T}) \rightarrow x^{(n)}(\mathcal{T})] = \min \left\{ 1, \frac{\mathcal{P}_{AB}[x^{(n)}(\mathcal{T})] P_{\text{gen}}[x^{(n)}(\mathcal{T}) \rightarrow x^{(o)}(\mathcal{T})]}{\mathcal{P}_{AB}[x^{(o)}(\mathcal{T})] P_{\text{gen}}[x^{(o)}(\mathcal{T}) \rightarrow x^{(n)}(\mathcal{T})]} \right\}. \quad (24)$$

Since the old trajectory  $x^{(o)}(\mathcal{T})$  is reactive, i.e.  $h_A[x_0^{(o)}] = 1$  and  $h_B[x_T^{(o)}] = 1$ , this acceptance probability can be written as:

$$\begin{aligned} P_{\text{acc}}[x^{(o)}(\mathcal{T}) \rightarrow x^{(n)}(\mathcal{T})] &= h_A[x_0^{(n)}] h_B[x_T^{(n)}] \\ &\times \min \left\{ 1, \frac{\mathcal{P}[x^{(n)}(\mathcal{T})] P_{\text{gen}}[x^{(n)}(\mathcal{T}) \rightarrow x^{(o)}(\mathcal{T})]}{\mathcal{P}[x^{(o)}(\mathcal{T})] P_{\text{gen}}[x^{(o)}(\mathcal{T}) \rightarrow x^{(n)}(\mathcal{T})]} \right\}. \end{aligned} \quad (25)$$

In practice, the Metropolis rule is implemented in the following way. First, the new path is generated. If the new path is not reactive, it is rejected. Otherwise, the ratio  $\mathcal{P}[\text{n}] P_{\text{gen}}[\text{n} \rightarrow \text{o}] / \mathcal{P}[\text{o}] P_{\text{gen}}[\text{o} \rightarrow \text{n}]$  is computed. If this ratio is larger

than one, the new path is accepted. If it is smaller than one, the new path is accepted only if a random number drawn from a uniform distribution in the interval  $[0, 1]$  is smaller than the ratio. Otherwise the path is rejected. In the case of a rejection the old path is retained as the current one. Repetition of this basic combination of generation and acceptance/rejection step yields a random walk through trajectory space that visits pathways according to their weight in the transition path ensemble.

### 3.2 Shooting and Shifting

In the preceding section we have laid out the general Monte Carlo procedure in trajectory space, but we have not yet specified how new pathways are generated from old ones. The efficiency of a transition path sampling simulation crucially depends on how this is done. A variety of schemes to do that exist [12], but so far the shooting algorithm has proven to be the most efficient one. For this reason and since the shooting algorithm is the only algorithm applicable to deterministic dynamics, we will discuss only this algorithm in detail (together with the complementary shifting procedure) and refer the reader to [12] for other path generating procedures. The rather detailed discussion of the shooting move may also serve as an illustration of how the general Monte Carlo formalism needs to be applied to derive appropriate acceptance probabilities for specific path moves.

The basic idea of the shooting algorithm is to generate pathways by using the propagation rules of the underlying dynamics. This is done by “shooting off” a new pathway from a randomly selected time slice  $x_{t'}^{(o)}$  along the old path. Before shooting this time slice may be modified yielding  $x_{t'}^{(n)}$  (this step is necessary for deterministic dynamics). From this perturbed time slice at time  $t'$  two new path segments are generated forward to time  $T$  and backward to time 0 according to the rules of the underlying dynamics. Together these two new segments form the new pathway (see Fig. 4). Since this shooting procedure is done stepwise the corresponding generation probabilities for the forward and backward path segments are:

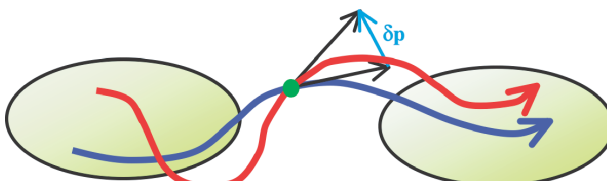


**Fig. 4.** In a shooting move for Newtonian dynamics a new path (dark gray) is created from an old one (light gray) by perturbing the momenta at a randomly selected time slice. From this perturbed point the equations of motion are then integrated backward and forward in time

$$P_{\text{gen}}^{\text{f}}[x^{\text{o}}(\mathcal{T}) \rightarrow x^{\text{n}}(\mathcal{T})] = \prod_{i=t'/\Delta t}^{\mathcal{T}/\Delta t - 1} p(x_{i\Delta t}^{\text{n}} \rightarrow x_{(i+1)\Delta t}^{\text{n}}) . \quad (26)$$

and

$$P_{\text{gen}}^{\text{b}}[x^{\text{o}}(\mathcal{T}) \rightarrow x^{\text{n}}(\mathcal{T})] = \prod_{i=1}^{t'/\Delta t} \bar{p}(x_{i\Delta t}^{\text{n}} \rightarrow x_{(i-1)\Delta t}^{\text{n}}) . \quad (27)$$

Since to generate the forward segment the dynamical rule of the underlying dynamics is used, (26) is just the dynamical path weight for the forward trajectory. For the backward move a time inverted transition probability  $\bar{p}(x \rightarrow x')$  is used. (The choice of the backwards propagation rule is obvious for most systems, but difficulties may arise in some non-equilibrium cases [12].) Combining the forward and backward generation probabilities one obtains the generation probability for the entire shooting move:

$$\begin{aligned} P_{\text{gen}}[x^{\text{o}}(\mathcal{T}) \rightarrow x^{\text{n}}(\mathcal{T})] &= p_{\text{gen}}[x_{t'}^{\text{o}} \rightarrow x_{t'}^{\text{n}}] \prod_{i=t'/\Delta t}^{\mathcal{T}/\Delta t - 1} p(x_{i\Delta t}^{\text{n}} \rightarrow x_{(i+1)\Delta t}^{\text{n}}) \\ &\times \prod_{i=1}^{t'/\Delta t} \bar{p}(x_{i\Delta t}^{\text{n}} \rightarrow x_{(i-1)\Delta t}^{\text{n}}) , \end{aligned} \quad (28)$$

where  $p_{\text{gen}}[x_{t'}^{\text{o}} \rightarrow x_{t'}^{\text{n}}]$  is the probability to obtain the *shooting point*  $x_{t'}^{\text{n}}$  by modification of state  $x_{t'}^{\text{o}}$ . (In the following we assume this generating probability for the shooting point to be symmetric. If it is not, this must be explicitly taken into account in the acceptance probability.) The generation probability (28) can now be used to derive an acceptance probability for pathways generated with the shooting algorithm.

$$\begin{aligned} P_{\text{acc}}[x^{\text{o}}(\mathcal{T}) \rightarrow x^{\text{n}}(\mathcal{T})] &= h_A[x_0^{\text{n}}] h_B[x_{\mathcal{T}}^{\text{n}}] \\ &\times \min \left[ 1, \frac{\rho(x_0^{\text{n}})}{\rho(x_0^{\text{o}})} \prod_{i=0}^{t'/\Delta t - 1} \frac{p(x_{i\Delta t}^{\text{n}} \rightarrow x_{(i+1)\Delta t}^{\text{n}})}{\bar{p}(x_{(i+1)\Delta t}^{\text{n}} \rightarrow x_{i\Delta t}^{\text{n}})} \times \frac{\bar{p}(x_{(i+1)\Delta t}^{\text{o}} \rightarrow x_{i\Delta t}^{\text{o}})}{p(x_{i\Delta t}^{\text{o}} \rightarrow x_{(i+1)\Delta t}^{\text{o}})} \right] . \end{aligned} \quad (29)$$

In this expression, all terms stemming from the forward segment have cancelled because the generation probability of the forward shot is identical to the dynamical path probability. Such a cancellation of terms does not occur for the backwards segment, because the corresponding generation probability  $\bar{p}(x \rightarrow x')$  is not a priori related in any simple way to the corresponding dynamical path probability. The acceptance probability (29), however, simplifies considerably if  $p$  and  $\bar{p}$  obey a microscopic reversibility condition with respect to the distributions of initial conditions:

$$\frac{p(x \rightarrow y)}{\bar{p}(y \rightarrow x)} = \frac{\rho_0(y)}{\rho_0(x)} . \quad (30)$$

A backward generation probability  $\bar{p}$  satisfying this condition can be constructed in many cases, in particular in equilibrium situations. If condition (30) holds, the acceptance probability for the shooting move becomes:

$$P_{\text{acc}}[x^{(o)}(\mathcal{T}) \rightarrow x^{(n)}(\mathcal{T})] = h_A[x_0^{(n)}]h_B[x_T^{(n)}] \min \left[ 1, \frac{\rho(x_{t'}^{(n)})}{\rho(x_{t'}^{(o)})} \right]. \quad (31)$$

Hence, any new path connecting the stable states  $A$  and  $B$  is accepted with a probability depending only on the shooting points of the old and the new pathway. This simple acceptance rule also suggests the following algorithm. First a shooting point  $x_{t'}^{(o)}$  is selected at random and modified to  $x_{t'}^{(n)}$ . Then, this shooting point is accepted if a random number selected from a uniform distribution in the interval  $[0, 1]$  is smaller than  $\rho(x_{t'}^{(n)})/\rho(x_{t'}^{(o)})$ . If the shooting point is accepted, either one of the path segments is grown. If this segment reaches the appropriate stable region, the other segment is grown. The whole path is finally accepted if the boundary condition for that segment is also satisfied. If any of these steps is rejected, the procedure must be started over.

The acceptance rule (31) is very general and valid for any procedure that is microscopically reversible in the sense of (30). Cases in which its is applicable include Langevin dynamics, Monte Carlo dynamics and Newtonian dynamics [12]. Since Newtonian dynamics is the arguably most important of these (most MD simulations are based on Newton's equations of motion), we next discuss the shooting algorithm for this case with initial conditions distributed according to the equilibrium phase space density. Extensions for other kinds of deterministic dynamics such as Nose-Hoover or Gaussian isokinetic dynamics can be easily derived from the general procedure presented above.

To carry out a shooting move for Newtonian dynamics, a procedure to generate the shooting point  $x_{t'}^{(n)}$  from the time slice  $x_{t'}^{(o)}$  has to be specified. In general, one can do that in a symmetric way by adding a perturbation  $\delta x$  to  $x_{t'}^{(o)}$ ,

$$x_{t'}^{(n)} = x_{t'}^{(o)} + \delta x. \quad (32)$$

The perturbation  $\delta x$  is drawn from a symmetric distribution, such that the generation probability for the new shooting point  $x_{t'}^{(n)}$  is symmetric with respect to the reverse move,  $p_{\text{gen}}(x_{t'}^{(o)} \rightarrow x_{t'}^{(n)}) = p_{\text{gen}}(x_{t'}^{(n)} \rightarrow x_{t'}^{(o)})$ . Symmetric generation of the shooting point can be a subtle issue, especially when there are rigid constraints. Methods for generating such displacements are discussed in [12].

In most cases, it is sufficient to change only the momentum part of the selected time slice  $x_{t'}^{(o)}$  while the configurational part is left unchanged, i.e.,  $p_{t'}^{(n)} = p_{t'}^{(o)} + \delta p$  and  $r_{t'}^{(n)} = r_{t'}^{(o)}$ . However, in some cases it is advantageous to change both the configuration and momentum parts of  $x_{t'}^{(o)}$  [26]. After generation of the shooting point the new trajectory is grown by applying dynamical propagation rules. For Newtonian dynamics this amounts to integrating the

equations of motion. While the forward segments of the trajectory can be generated by carrying out the appropriate number of small time steps in forward direction, the backward segment has to be generated with inverted time direction, i.e., with a negative time step. Since Newton's equation of motion are time reversible, backward trajectory segments may be obtained by first inverting all momentum-like variables, and then integrating as if forward in time. Momenta in the resulting chain of states are then inverted to give the proper direction of time. To check whether this procedure satisfies the reversibility criterion (30) we consider the forward and backward transition probabilities for a short time step,

$$p(x \rightarrow y) = \delta[y - \phi_{\Delta t}(x)], \quad (33)$$

and

$$\bar{p}(y \rightarrow x) = \delta[x - \phi_{-\Delta t}(y)] = \delta[x - \phi_{\Delta t}^{-1}(y)]. \quad (34)$$

For Dirac delta-functions the following equality is valid,

$$\delta[y - \phi_{\Delta t}(x)] = \delta[\phi_{\Delta t}^{-1}(y) - x] |\partial\phi_{\Delta t}(x)/\partial x|^{-1}, \quad (35)$$

where  $|\partial\phi_{\Delta t}(x)/\partial x|$  is the Jacobian factor associated with the time evolution for a time step  $\Delta t$ . This Jacobian describes the contraction or expansion of an infinitesimal comoving volume element in phase space. Consequently, the single step forward and backward generation probabilities are related by

$$\frac{p(x \rightarrow y)}{\bar{p}(y \rightarrow x)} = \left| \frac{\partial\phi_{\Delta t}(x)}{\partial x} \right|^{-1}. \quad (36)$$

Since the phase space flow conserves the equilibrium distribution, we also have

$$\rho_0(\phi_{\Delta t}(x)) = \rho_0(x) \left| \frac{\partial\phi_{\Delta t}(x)}{\partial x} \right|^{-1}. \quad (37)$$

Hence, condition (30) holds and pathways generated with this algorithm can be accepted with the probability (31). For a microcanonical distribution of initial conditions together with Newtonian dynamics care must be taken that the perturbation of the shooting point does not change the energy. Algorithms to do that in a symmetric way are available [12]. In this case the acceptance probability further simplifies to

$$P_{\text{acc}}[x^{(o)}(\mathcal{T}) \rightarrow x^{(n)}(\mathcal{T})] = h_A[x_0^{(n)}]h_B[x_{\mathcal{T}}^{(n)}]. \quad (38)$$

In words, any new pathway that starts in  $A$  and ends in  $B$  is accepted. All other pathways must be rejected. Shooting moves can be complemented with shifting moves (see Fig. 5). In this computationally inexpensive move a new path is generated from an old one by translating the trajectory forward or backward in time. More specifically, in a forward shifting move a trajectory



**Fig. 5.** In a shifting move for Newtonian dynamics a new path (*dark gray*) is created from an old one (*light gray*) by translating the initial point of the trajectory forward in time (such as in the picture) or backward in time

segment of a certain length is first removed from the beginning of the path. Then, a segment of the same length is grown at the end of the path by integrating the equations of motion for an appropriate number of time steps starting from the final point of the old path. As a result of this procedure the new path overlaps partially with the old one. For a backward shifting move one proceeds in an analogous way. The shifting procedure effectively translates the path in time in a way reminiscent of the “reptation” motion of a polymer in a dense melt [27].

For Hamiltonian dynamics with a canonical or microcanonical distribution of initial conditions the acceptance probability for pathways generated with the shifting algorithm is particularly simple. Provided forward and backward shifting moves are carried out with the same probability, the acceptance probability reduces to [12]

$$P_{\text{acc}}[x^{(\text{o})}(\mathcal{T}) \rightarrow x^{(\text{n})}(\mathcal{T})] = h_A[x_0^{(\text{n})}]h_B[x_t^{(\text{n})}] . \quad (39)$$

implying that any new path that still connects regions  $A$  and  $B$  is accepted. Similarly, simple acceptance probabilities can be derived also for pathways generated with stochastic instead of deterministic dynamics [12]. Although new pathways generated by the shifting algorithm differ little from the corresponding old pathways especially in the transition region, shifting moves can improve the convergence of averages taken over the transition path ensemble.

### 3.3 Generating an Initial Path

To start a transition path sampling simulation with the algorithms described above an initial pathway connecting  $A$  with  $B$  must be available. Hence, generating an initial transition pathway is an important step in the application of the transition path sampling methodology. In the simplest case an initial trajectory connecting  $A$  and  $B$  can be obtained by running a long molecular dynamics (or stochastic dynamics) simulation. For most applications, however, this straightforward approach is ruled out by the rarity of the event one wants to study and an initial trajectory has to be created artificially. The specific way to generate such a trajectory is highly system dependent, but in general one produces an atypical trajectory with a low weight in the transition path ensemble  $\mathcal{P}_{AB}[x(t)]$ . Therefore the first part of a transition path

sampling simulation starting from such a newly created trajectory consists of equilibrating the pathway towards the more important regions of trajectory space. This situation is analogous to that encountered in a conventional MC simulation of a molecular system. In that case a sufficiently long equilibration period is necessary to relax an unlikely initial configuration towards more probable regions of configuration space. Similarly, a transition path sampling simulation can start from an artificial pathway which does not even need to be a true dynamical trajectory. Then, repeated application of the Monte Carlo steps described above move the pathways towards more typical regions of pathways and the actual transition path sampling simulation can begin.

A more systematic way to create a new transition pathway is to gradually change the ensemble  $\mathcal{P}_{AB}[x(t)]$  from one which includes all trajectories starting in  $A$  (without restrictions on the end point) to one which consists only of trajectories starting in  $A$  and ending in  $B$ . As will be discussed in Sect. 5, conversion of one path ensemble into another is computationally demanding and in most cases more efficient ways to generate an initial trajectory exist.

In some situations, high-temperature pathways can be used to initiate a transition path sampling simulation. Consider, for example, the folding/unfolding of a protein. At physiological temperatures, a protein in its native states unfolds only very rarely on a molecular time scale. At higher temperatures, however, unfolding occurs so quickly that it can be simulated with ordinary molecular dynamics simulations. Such a high temperature trajectory can then be used to start a transition path sampling simulation at the temperature of interest. If high temperature transition pathways are qualitatively very different from those at lower temperatures it might be necessary to carry out a systematic cooling procedure, in which the ensemble of pathways if brought to lower temperature in small steps.

In other cases, one may have some, possibly incomplete notion of a reaction coordinate. Controlling this presumed reaction coordinate one might be able to drive the system from  $A$  to  $B$  obtaining a chain of states from which shooting and shifting moves can be initiated. In our experience no general recipe exists for the generation of an initial trajectory. Rather, specific procedures have to be developed for this purpose for each application of the transition path sampling method to a new problem.

## 4 Reaction Mechanisms: Analyzing Transition Pathways

The path ensemble, as created by the transition path sampling methodology, is a statistically representative collection of trajectories leading from a reactant region to a product region. Further analysis of this ensemble of pathways is necessary to obtain rate constants, reaction mechanisms, reaction coordinates, transition state structures etc. In this section we will describe how to analyze the path ensemble by determining transition state ensembles, and how to test proposed reaction coordinates using *committor* distributions.

#### 4.1 Reaction Coordinate vs. Order Parameter

The application of the transition path sampling formalism requires a proper definition of the stable states  $A$  and  $B$ . This can be achieved using so called *order parameters*, variables that discriminate configurations belonging to the reactant region from those in the product region. Such order parameters, however, are not necessarily suitable for the characterization of the reaction mechanism. To emphasize this fact we distinguish the term *order parameter* from the term *reaction coordinate*, which is a variable capable of describing the dynamical bottleneck separating products from reactants. This distinction is illustrated schematically in Fig. 6. Along a good reaction coordinate the system can be driven reversibly from one state to the other because all degrees of freedom orthogonal to the reaction coordinate equilibrate quickly. Driving the system from  $A$  to  $B$  by controlling the wrong coordinate, on the other hand, leads to large hysteresis effects because such a procedure neglects important barriers that may exist in orthogonal directions. A good reaction coordinate should capture the essence of the dynamics and allow us to predict what a trajectory starting from a given configuration will most likely do. As we will see later, this is exactly what the committor does: it tells us about the probability to relax into  $A$  or  $B$ . Thus, if a good reaction coordinate is available, the committor can be parametrized in terms of this coordinate [28].

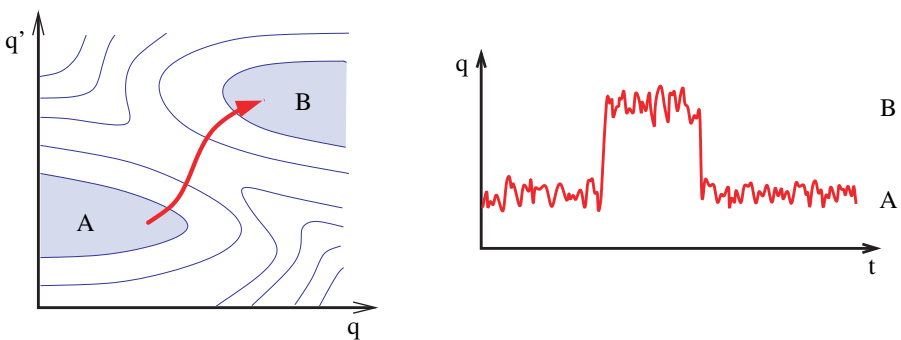


**Fig. 6.** Free energy landscape in which during a transition from  $A$  to  $B$  both the variable  $q$  and  $q'$  change systematically (*left hand side*). For this case, the variable  $q$  is a good order parameter and suffices to distinguish the equilibrium fluctuations in the stable states  $A$  and  $B$ . By following  $q$  as a function of time  $t$  we can detect transitions between the stable states (*right hand side*). However, this variable does not capture all essential aspects of the transition and is therefore not a good reaction coordinate. In the definition of such a good reaction coordinate capable of describing the complete course of the reaction the variable  $q'$  can not be neglected

## 4.2 Committor

In the analysis of chemical dynamics the transition state plays a prominent role. Usually, the transition state is identified with saddle points of the potential energy surface where forces vanish and there is exactly one unstable mode. A system resting on a saddle point is an unstable state that can evolve either to the reactants or the products depending on which side we kick it. The concept of a transition state can be generalized and quantified for arbitrary configurations by considering the probability to proceed to reactants or products after averaging over noise and/or initial velocities. Onsager called this probability the *splitting probability* and used it to investigate ion-pair recombination [29] and in protein folding studies the term  $p_{\text{fold}}$  is used [30]. Here, we will call this relaxation probability the *committor*, because it tells us with which likelihood a certain configuration is committed to one of the two stable states (usually state  $B$ ). The committor is a direct statistical indicator of the progress of the reaction. In this sense it is an ideal reaction coordinate. Parametrizing the committor in terms of small number of atomic variables to gain insight into the reaction mechanism, however, is a highly non-trivial task.

For a given configuration  $r$  the committor is defined as the fraction of trajectories started in  $A$  that reach stable state  $B$  after time  $t$ ,

$$p_B(r, t) \equiv \frac{\int \mathcal{D}x(t) \mathcal{P}[x(t)] \delta(r_0 - r) h_B(x_t)}{\int \mathcal{D}x(t) \mathcal{P}[x(t)] \delta(r_0 - r)}, \quad (40)$$

where  $r_0$  is the initial configuration of the system from which the trajectory  $x(t)$  is integrated (see Fig. 7). For Newtonian dynamics and a canonical distribution of initial conditions the average in the above expression is over all momenta distributed according to a Maxwell-Boltzmann distribution. For stochastic dynamics the average extends also over noise histories. The committor is a statistical measure for how *committed* a given configuration is to the product state. A value of  $p_B = 0$  indicates no commitment at all while a value of

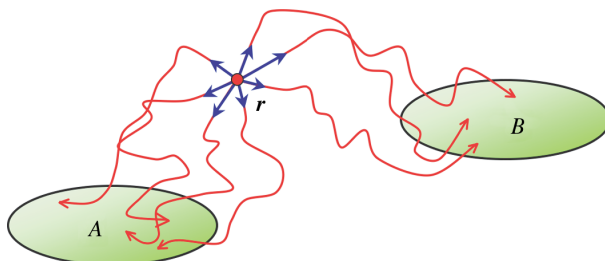


**Fig. 7.** For a given configuration  $r$  the committor  $p_B(r)$  is calculated by initiating many trajectory with random momenta from  $r$ . Each trajectory is then propagated for a time  $t$ . The committor  $p_B$  is estimated from the fraction of trajectories that reach  $B$  in the time  $t$

$p_B = 1$  that the configuration is fully committed to  $B$ . Configurations with  $p_A \approx p_B$  are committed neither to  $A$  nor to  $B$ . Note the committor as defined above depends on time. This time has to be selected such that it is larger than the molecular time scale  $\tau_{\text{rxn}}$  discussed in Sect. 5. A time-independent form of the committor can be defined by counting all trajectories originating from a given configuration  $r$  that reach state  $B$  before they reach state  $A$  [8]. In a practical calculation, only a finite sample of trajectories is available to determine the committor:

$$p_B(r, t) \approx \frac{1}{N} \sum_{i=1}^N h_B(x_t^{(i)}) \equiv p_B^{(N)}(r, t). \quad (41)$$

Assuming that the  $N$  trajectories are statistically independent, the standard deviation of  $p_B$  calculated from  $N$  trajectories is:

$$\sigma = \sqrt{\langle (p_B^{(N)} - p_B)^2 \rangle} = \sqrt{\frac{p_B(1 - p_B)}{N}}. \quad (42)$$

This expression can be used to terminate a committor calculation after a certain desired accuracy has been reached. The largest number of trajectories is needed for configurations with a committor of  $p_B \approx 1/2$ .

### 4.3 The Transition State Ensemble

We define a configuration  $r$  to be a transition state (TS), if both stable states  $A$  and  $B$  are equally accessible from that configuration (see Fig. 8). In other words,  $r$  is a transition state if

$$p_A(r) = p_B(r). \quad (43)$$

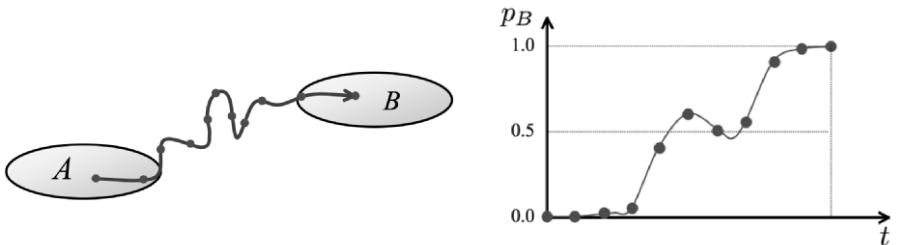


**Fig. 8.** The committor calculated for points along a path connecting the stable states  $A$  and  $B$  is a function which grows from  $p_B = 0$  at configuration lying in and near  $A$  to  $p_B = 1$  for configurations in  $B$  or nearby. In between, the committor will take the value  $p_B = 0.5$  at least once but possibly several times. Configurations with  $p_A = p_B = 0.5$  are equally likely to relax into either one of the stable states. We define these configurations to be the transition states

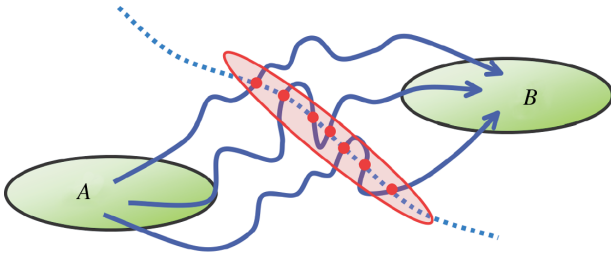


**Fig. 9.** All configurations on transition pathways that have a committor of  $p_B = 0.5$  are members of the *transition state ensemble*. Each transition path contributes at least one configuration but possibly more to the transition state ensemble. The dashed line is the separatrix (or isocommittor 1/2 surface)

Transition states defined in this statistical way do not necessarily coincide with particular features of the potential energy surface. In certain cases, such as the diffusion of adatoms on solids at low temperature, points with  $p_A(r) = p_B(r)$  may be located at or near saddle points of the potential energy surface, but in general entropic contributions play an important role in determining the location of statistically defined transition states in configuration space. For instance, the transition from a hard sphere fluid to a hard sphere solid proceeds through a purely entropic transition state [31]. Equation (43) defines a surface separating the basins of attraction of the stable states. This dividing surface is also called the *separatrix*. If all trajectories started from configuration  $r$  end either in  $A$  or in  $B$  then  $p_A(r) + p_B(r) = 1$ . In this case a transition state is characterized by  $p_A = p_B = 1/2$ . To find configurations belonging to the separatrix one can locate configurations with  $p_A = p_B$  on transition pathways. The set of all such configurations is the *transition state ensemble* (see Fig. 9). This operation introduces a weight on the separatrix. Analysis of the transition state ensemble can yield important information about the reaction mechanism.

#### 4.4 Committor Distributions

Consider the situation illustrated in Fig. 10 for proton transfer in the protonated water trimer. Suppose one has postulated the variable  $\Delta r$  as the reaction coordinate for the transition. Then, the question arises if  $\Delta r$  is a relevant and sufficient description of the reaction mechanism. In the case of the Fig. 10 it is clearly not. If one drives the transition by controlling  $\Delta r$ , hysteresis will occur, indicating that the variable  $\Delta r$  is not sufficient for a dynamical description of the reaction. Observing hysteresis is a crude way of testing reaction coordinates and a more precise procedure is called for. Calculating distributions of committors for constraint ensembles can be precisely the powerful tool we need to test the correctness of the proposed reaction coordinate. This diagnostic tool is not restricted to TPS but can be applied

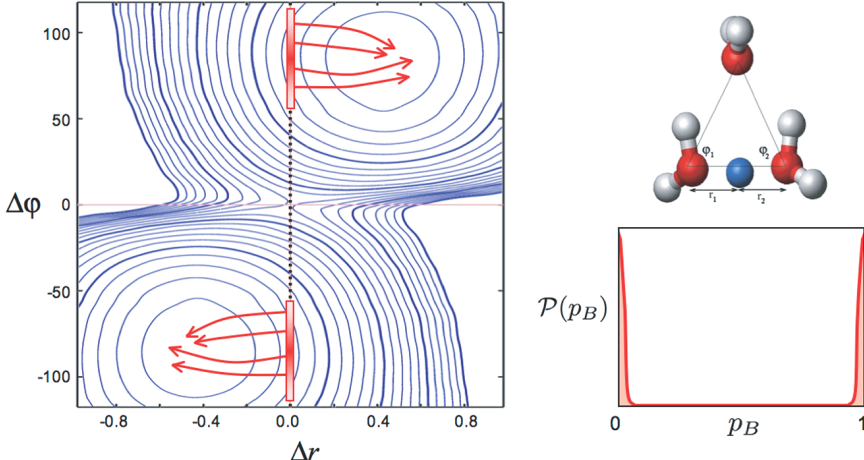


**Fig. 10.** If in the case of the protonated water trimer trajectories are started from configurations in which the proton coordinate  $\Delta r = r_2 - r_1$  vanishes (all other variables are distributed according to the equilibrium distribution), the proton always relaxes to one of the two stable states. To which one depends on the values of the angular variable  $\Delta\varphi = \varphi_2 - \varphi_1$  describing the geometry of the OOO-triangle. For initial conditions located in the lower red stripe in the free energy landscape on the left hand side, the proton will always relax into the state characterized by negative values of  $\Delta\varphi$ . Trajectories started in the upper red stripe will always evolve towards the other stable state with positive values of  $\Delta\varphi$ . The distribution  $P(p_B)$  obtained by repeated calculation of the committor  $p_B$  will hence show a sharp peak at  $p_B = 0$  and another sharp peak at  $p_B = 1$ . In general such a result indicates that degrees of freedom important for the analysis have been neglected. In the case of the protonated water trimer this degree of freedom is the angular difference  $\Delta\varphi$

to any case requiring a test whether or not the proposed order parameter describes the transition or is only partially correlated (if at all) with the reaction coordinate.

The first step in this procedure is the calculation of the free energy profile as a function of a variable  $q$  (in the case of the protonated trimer this is  $\Delta r$ ). If  $q$  differs in the reactant and product region, the free energy as a function of  $q$  will most likely show a barrier with maximum at  $q = q^*$ . Next, configurations with  $q = q^*$  are generated, for instance by imposing constraints in a molecular dynamics simulation [32]. Subsequently, commitment probabilities are computed for a representative number of configurations in this ensemble. If each of these configurations is truly in the transition state region, the committors will be around  $p_B = 0.5$ . If, in contrast, they are far from one half, say 0 or 1, the configurations are clearly not part of the separatrix. Hence, they cannot be transition states in the sense we discussed in the previous section.

To analyze this situation further we construct a histogram of the committors, a committor distribution  $P(p_B)$ ,

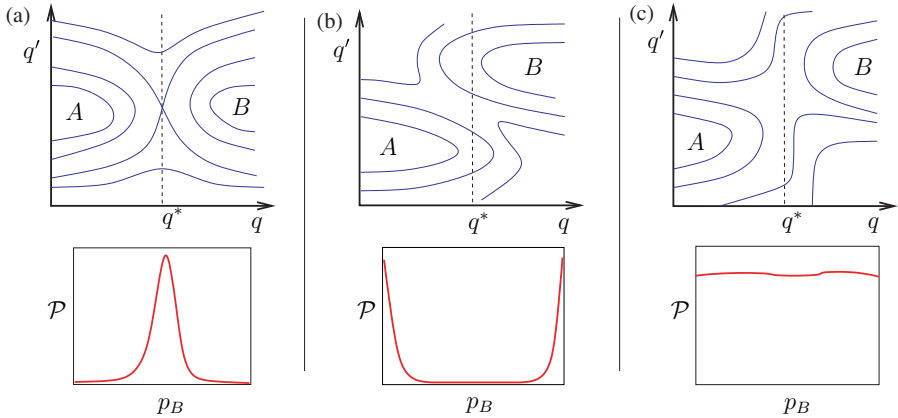


**Fig. 11.** Three scenarios leading to different committor distributions. **(a)** The variable  $q$  is a good reaction coordinate. Configurations constrained at  $q = q^*$  produce a distribution of committors peaked at  $p_B = 0.5$ . **(b)** The variable  $q$  is insufficient to describe the reaction properly. As a result the committor distribution for configurations with  $q = q^*$  is peaked at zero and unity. For a correct description of the transition the variable  $q'$  must be taken into account. **(c)** The transition occurs diffusively in the direction of  $q'$ . In this case the committor distribution is flat

$$P(\tilde{p}_B) = \frac{\langle \delta[\tilde{p}_B - p_B(r, t)]\delta[q^* - q(r)] \rangle}{\langle \delta[q^* - q(r)] \rangle}. \quad (44)$$

Here,  $P(p_B)$  is the probability (density) for finding the committor  $p_B$  in the ensemble  $q = q^*$ . If this distribution is peaked around  $p_B = 0.5$ , the constraint ensemble  $q = q^*$  is located on the separatrix and coincides with the transition state ensemble. In this case,  $q$  is a good reaction coordinate, at least in the neighborhood of the separatrix. This is illustrated in Fig. 11a. Other possible scenarios for the underlying free energy landscape result in different committor distributions, and are also illustrated in Fig. 11. The committor distribution can thus be used to estimate how far a postulated reaction coordinate is removed from the correct reaction coordinate. An application of this methodology can be found in [33], where the reaction coordinate of the crystallization of a Lennard-Jones fluid has been resolved by analysis of committor distributions.

## 5 Kinetics

Since pathways collected with transition path sampling are true dynamical trajectories rather than artificial sequences of states such as minimum energy pathways, they can be used to study the kinetics of the reaction. In the following we will first define reaction rate constants and explain how they are related

to the microscopic dynamics of the system. At the heart of this relation lie specific time correlation functions. Then, we will discuss several methods for calculating transition rate constants within the framework of transition path sampling. These methods use slightly different expressions, but all of them rely on efficient path sampling techniques.

### 5.1 Reaction Rate Constants and Population Fluctuations

Consider the unimolecular reaction



which interconverts molecules of type  $A$  and  $B$  into each other. At a given time  $t$  there are  $N_A(t)$  molecules of type  $A$  and  $N_B(t)$  molecules of type  $B$  in a container of volume  $V$ . The corresponding concentrations  $c_A(t) = N_A(t)/V$  and  $c_B(t) = N_B(t)/V$  can change in time due to molecules undergoing the reaction. Since according to the assumption molecules can only interconvert into each other, the total number of molecules is constant,  $N_A(t)+N_B(t) = N$ . Provided the solution is sufficiently dilute, i.e., the molecules are independent from each other, the time evolution of the concentrations can be described on a phenomenological level by the rate equations

$$\begin{aligned} \dot{c}_A &= -k_{AB} c_A + k_{BA} c_B, \\ \dot{c}_B &= k_{AB} c_A - k_{BA} c_B . \end{aligned} \quad (46)$$

Here,  $k_{AB}$  and  $k_{BA}$  are the forward and backward reaction rate constants, respectively. These are the quantities that we want to calculate with transition path sampling. To solve the kinetic equations (46) it is convenient to consider the deviation of the concentrations from their equilibrium value:

$$\begin{aligned} \Delta c_A(t) &= c_A(t) - \langle c_A \rangle \\ \Delta c_B(t) &= c_B(t) - \langle c_B \rangle , \end{aligned} \quad (47)$$

where  $\langle c_A \rangle$  and  $\langle c_B \rangle$  are the concentrations one finds when equilibrium sets in. Since  $\Delta c_A(t) = -\Delta c_B(t)$  it is sufficient to consider only  $\Delta c_A(t)$ . According to the analytical solution of the rate equations  $\Delta c_A(t)$  decays exponentially from its initial value  $\Delta c_A(0)$ ,

$$\Delta c_A(t) = \Delta c_A(0) \exp(-t/\tau_{\text{rxn}}) . \quad (48)$$

The *reaction time*  $\tau_{\text{rxn}}$  depends on the forward and backward reaction rate constants,

$$\tau_{\text{rxn}}^{-1} = k_{AB} + k_{BA} . \quad (49)$$

If the reaction rate constants for the forward and backward reactions differ considerably, the reaction time is dominated by the larger rate constant. The

above solution of the rate equations describes how a non-equilibrium concentration decays towards its equilibrium value. The description of the reaction in terms of kinetic equations is purely phenomenological and does not make any reference to the molecular nature of the system. To calculate the kinetic coefficients  $k_{AB}$  and  $k_{BA}$  from an atomistic theory we need to compare the time evolution (48) predicted by the kinetic equations (46) with the time evolution observed in the microscopic picture. Usually, such a comparison is carried out in the framework of linear response theory, in which one considers the response of the system to small perturbations of the concentrations [34]. Here, we connect the microscopic with the macroscopic picture following a slightly different approach. Rather than considering *small* perturbations we study the response of the system to *large* changes in the concentrations. Remarkably, both approaches yield identical expressions for the reaction rate constants. The reason for this agreement is that for the systems considered here the full response to a perturbation of arbitrary strength, just as the linear response, is fully determined by the equilibrium fluctuations of the system. This is explained in detail in the Appendix.

To derive microscopic expressions for the reaction rate constants we first use the solution of the rate equations to determine the fraction of molecules of type  $B$  at time  $t$  under the condition that initially all of the  $N$  molecules were of type  $A$ , i.e.  $N_A(0) = N$  and  $N_B(0) = 0$ ,

$$\frac{N_B(t)}{N} = \frac{\langle N_B \rangle}{N} \left( 1 - e^{-t/\tau_{\text{rxn}}} \right), \quad (50)$$

where  $\langle N_B \rangle$  is the number of molecules of type  $B$  in equilibrium. This fraction is nothing else than the conditional probability to find a molecule in state  $B$  at time  $t$  provided it was in state  $A$  at time 0:

$$P(B, t | A, 0) = \frac{\langle N_B \rangle}{N} \left( 1 - e^{-t/\tau_{\text{rxn}}} \right). \quad (51)$$

We will now make contact with the microscopic picture by calculating this conditional probability from the microscopic dynamics of the system. Since by assumption the molecules are independent from each other, it is sufficient to follow the time evolution of a single molecule. For this molecule the characteristic functions  $h_A(x)$  and  $h_B(x)$  introduced earlier serve to distinguish between state  $A$  and  $B$ . The characteristic functions usually depend only on structural properties such as angles, distances or other geometric criteria, but for generality we write  $x$ , the full states of the system in phase space, as their argument. By calculating  $h_A$  and  $h_B$  for a particular state  $x$  we can tell whether the molecule is of type  $A$  or  $B$ . Here we do not assume that the molecule is either in  $A$  or in  $B$  at all times, i.e.,  $h_A(x) + h_B(x)$  is not necessarily unity for all configurations. But if states  $A$  and  $B$  are stable and the characteristic functions are defined properly,  $h_A(x) + h_B(x) = 1$  most of the time. Only for short times, for instance during a transition from  $A$  to  $B$ , we can have  $h_A(x) + h_B(x) = 0$ .

To calculate the conditional probability  $P(B, t|A, 0)$  from the microscopic dynamics of the system we imagine that we prepare initial conditions  $x_0$  according to the equilibrium distribution  $\rho(x_0)$  but restricted to the reactant region  $A$ ,

$$\rho_A(x_0) = \rho(x_0)h_A(x_0)/Z_A , \quad (52)$$

where

$$Z_A = \int dx_0 \rho(x_0)h_A(x_0) \quad (53)$$

normalizes this restricted distribution. We now follow the time evolution of the system starting from many of such initial conditions in  $A$  and observe if the system is in  $B$  after time  $t$  by calculating  $h_B(x_t)$ . Averaging over all initial conditions  $x_0$  with the appropriate weight yields the conditional probability to find the system in  $B$  at time  $t$  given that it was in  $A$  at time 0,

$$P(B, t|A, 0) = \int dx_0 \rho_A(x_0)h_B(x_t) = \frac{\int dx_0 \rho(x_0)h_A(x_0)h_B(x_t)}{\int dx \rho(x_0)h_A(x_0)} . \quad (54)$$

Denoting averages over the equilibrium distribution (and possibly over the noise history) by  $\langle \dots \rangle$  we can also write

$$P(B, t|A, 0) = \frac{\langle h_A(x_0)h_B(x_t) \rangle}{\langle h_A \rangle} , \quad (55)$$

where  $\langle h_A(x_0)h_B(x_t) \rangle$  is a so called time correlation function and  $\langle h_A \rangle$  is the average value of  $h_A(x)$ , i.e., the fraction of molecules of type  $A$  in equilibrium.

Equation (55), expressing the conditional probability  $P(B, t|A, 0)$  in terms of a time correlation function, now permits to link the phenomenological and microscopic descriptions. By equating (51) and (55) and by noting that  $\langle N_B \rangle/N = \langle h_B \rangle$  we find that

$$\frac{\langle h_A(x_0)h_B(x_t) \rangle}{\langle h_A \rangle} = \langle h_B \rangle \left( 1 - e^{-t/\tau_{\text{rxn}}} \right) . \quad (56)$$

While the left hand side of this equation is purely microscopic, the right hand side originates from the solution of the phenomenological rate equations. Relation (56) provides the link we were looking for.

Since the rate equations (46) treat transitions at a very coarse grained level and neglect all microscopic details of the transition, (56) cannot hold at all times. Particularly for short times deviations are expected. This does, however, not imply that the phenomenological description is incorrect but only limits its range of validity. For times that are long compared to  $\tau_{\text{mol}}$ , the time scale of molecular correlations, this relation should hold. The situation is similar to that encountered in the context of diffusion. While the (phenomenological) diffusion equation predicts a linear dependence of the mean squared displacement on time, microscopic dynamics yields a quadratic dependence for short times (ballistic regime). Only after a transient time, the length of

which is determined by the persistence of correlations, does linear behavior set in.

To analyze (56) further let us assume that the reaction time  $\tau_{\text{rxn}}$  is much longer than the molecular time scale  $\tau_{\text{mol}}$  (this is exactly the situation we are interested in). Then, for times  $\tau_{\text{mol}} < t \ll \tau_{\text{rxn}}$  a Taylor expansion of the right hand side yields

$$\frac{\langle h_A(x_0)h_B(x_t) \rangle}{\langle h_A \rangle} = \langle h_B \rangle \frac{t}{\tau_{\text{rxn}}} . \quad (57)$$

Exploiting that in equilibrium  $\langle h_A \rangle k_{AB} = \langle h_B \rangle k_{BA}$  [this detailed balance condition follows from the rate (46)] and noting that  $\tau_{\text{rxn}}^{-1} = k_{AB} + k_{BA}$  we finally find

$$C(t) \equiv \frac{\langle h_A(x_0)h_B(x_t) \rangle}{\langle h_A \rangle} = (\langle h_A \rangle + \langle h_B \rangle)k_{AB}t \approx k_{AB}t . \quad (58)$$

Thus, the slope of the time correlation  $C(t)$  in the time regime  $\tau_{\text{mol}} < t \ll \tau_{\text{rxn}}$  is the forward reaction rate constant  $k_{AB}$ . The function  $C(t)$  contains all the information needed to determine the reaction rate constant. Note that the relations obtained in this section can also be derived using linear response theory [34].

## 5.2 Free Energies in Path Space

To evaluate the time correlation function  $C(t)$  in the transition path sampling framework we rewrite it in terms of sums over trajectories:

$$C(t) = \frac{\int \mathcal{D}x(t) h_A(x_0) \mathcal{P}[x(t)] h_B(x_t)}{\int \mathcal{D}x(t) h_A(x_0) \mathcal{P}[x(t)]} = \frac{Z_{AB}(t)}{Z_A} . \quad (59)$$

This expression can be viewed as the ratio between the partition functions for two different path ensembles: in the denominator we have the partition functions for the set of pathways that start in  $A$  and end anywhere. The partition function in the numerator is the one for the ensemble of pathways that start in  $A$  and end in  $B$ . In a sense, this ratio of partition functions measures the volume in trajectory space occupied by reactive trajectories relative to that of the trajectories starting in  $A$  but without restriction on the ending point.

This perspective suggests to determine the correlation function  $C(t)$  via calculation of  $\Delta F(t) = F_{AB}(t) - F_A$ , the difference of the free energies related to the partition functions in the numerator and denominator. The free energy difference  $\Delta F$  can also be viewed as the work  $W_{AB}(t)$  necessary to convert the two ensembles *reversibly* into each other,

$$W_{AB}(t) \equiv -\ln \frac{Z_{AB}(t)}{Z_A} . \quad (60)$$

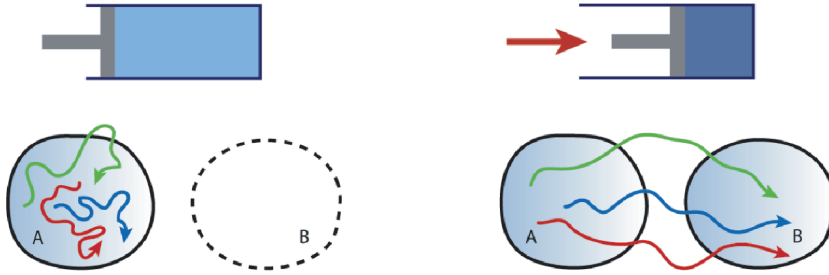


**Fig. 12.** Calculation of the time correlation function  $C(t)$  is equivalent to determining the reversible work  $W_{AB}(t)$  required to confine the endpoints of paths originating from region  $A$  into region  $B$ . This amounts to a “compression” of pathways in trajectory space

This is the work we need to “compress” the path ensemble and confine the endpoints of the paths with length  $t$  to the product region  $B$  (see Fig. 12). Note that  $W_{AB}(t)$  depends on the path length  $t$ . From the free energy difference one can than immediately determine the time correlation function,  $C(t) = \exp[-W_{AB}(t)]$ . Due to the formal similarity of free energies of ensembles of configurations and ensembles of trajectories, standard free energies estimation methods such as thermodynamic integration or umbrella sampling can be used for the calculation of  $W_{AB}(t)$  and hence of the time correlation function  $C(t)$ . In the following section we will discuss the application of the umbrella sampling technique [35] to this problem.

### 5.3 Umbrella Sampling

Umbrella sampling is a non-Boltzmann technique designed to enhance the sampling of rare but important regions of configuration space [35]. Here, we will apply it to enhance the sampling of rare but important regions in path space [36]. For this purpose we introduce an order parameter  $\lambda(x)$  that distinguishes between the reactant and product region. In other words, the range of values  $\lambda$  takes when the system is in  $A$ ,  $\lambda_{\min}^A < \lambda < \lambda_{\max}^A$ , does not overlap with the range of values  $\lambda$  takes in  $B$ ,  $\lambda_{\min}^B < \lambda < \lambda_{\max}^B$ . Let us also assume that  $\lambda_{\max}^A < \lambda_{\min}^B$ . Next, we consider the probability density for finding a particular value of the parameter  $\lambda$  at the endpoints of pathways starting in  $A$ :

$$P_A(\tilde{\lambda}, t) = \frac{\int \mathcal{D}x(t) h_A(x_0) \mathcal{P}[x(t)] \delta[\tilde{\lambda} - \lambda(x_t)]}{Z_A} = \langle \delta[\tilde{\lambda} - \lambda(x_t)] \rangle_A . \quad (61)$$

By integrating this distribution over the final region we obtain the conditional probability to find the system in  $B$  at time  $t$  provided its was in  $A$  at time 0,

$$C(t) = \exp[-W_{AB}(t)] = \int_{\lambda_{\min}^B}^{\lambda_{\max}^B} d\lambda P_A(\lambda, t) . \quad (62)$$

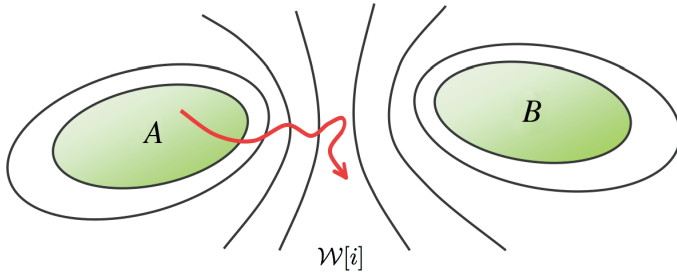


**Fig. 13.** In an umbrella sampling simulation for pathways configuration space is covered with a sequence of overlapping windows  $\mathcal{W}[i]$ . For each window a separate transition path sampling simulation for paths with starting points in  $A$  and endpoints in  $\mathcal{W}[i]$  is carried out. From the order parameter distributions matched where the windows overlap the distribution  $P_A(\lambda, t)$  can be calculated

In principle one could calculate the distribution (61) by generating initial conditions in  $A$  and histogram the values of  $\lambda$  at the endpoints of the trajectories started from these initial conditions. Since transitions from  $A$  to  $B$  are rare, however, such an approach fails to collect sufficient statistics in the  $\lambda$ -range corresponding to region  $B$ . Here, an umbrella sampling procedure can help. This is done by dividing the whole range of the parameter  $\lambda$  into overlapping windows. Each of these windows corresponds to a region  $\mathcal{W}[i]$  in phase space (see Fig. 13). For each window a separate path sampling simulation is carried out for the ensemble

$$\mathcal{P}_{AW[i]}[x(t)] = \rho(x_0)\mathcal{P}[x(t)]h_A(x_0)h_{\mathcal{W}[i]}(x_t), \quad (63)$$

in which pathways are required to start in  $A$  and end in window  $\mathcal{W}[i]$ . From these simulations the order parameter distribution in each window is computed:

$$\begin{aligned} P_{AW[i]}(\tilde{\lambda}, t) &= \frac{\int \mathcal{D}x(t) h_A(x_0)\mathcal{P}[x(t)]h_{\mathcal{W}[i]}(x_t)\delta[\tilde{\lambda} - \lambda(x_t)]}{\int \mathcal{D}x(t) h_A(x_0)h_{\mathcal{W}[i]}(x_t)} \\ &= \langle \delta[\tilde{\lambda} - \lambda(x_t)] \rangle_{AW[i]}. \end{aligned} \quad (64)$$

By matching these order parameter probabilities where the windows overlap one finally obtains the distribution  $P_A(\lambda, t)$  over the whole order parameter range. The results of an example calculation are shown in Fig. 14. Note that through this windowing procedure it is possible to calculate the distribution  $P_A(\lambda, t)$  even in the range where it is very small.

#### 5.4 Reversible Work to Change the Path Length

With the umbrella sampling procedure described in the previous paragraph it is possible to determine the time correlation function  $C(t)$  for different times

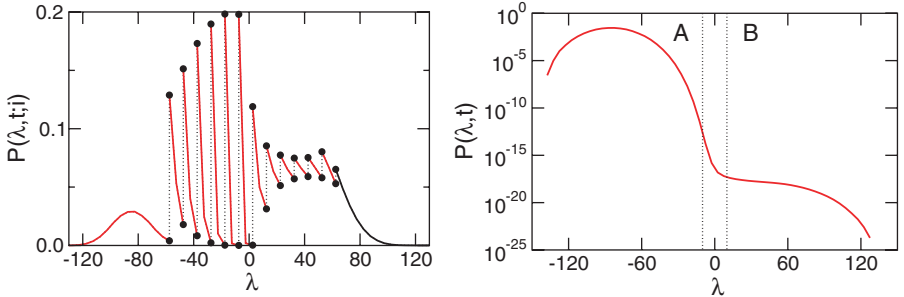


**Fig. 14.** Distribution of the order parameter  $\lambda$  in different order parameter windows for pathways of a given length  $t$  (*left hand side*). Matching the distributions in the windows where they overlap yields the distribution over the full order parameter range from the reactant region to the product region (*right hand side*). The data are from simulations of proton transfer in the protonated water trimer

$t$ . From a time derivative determined numerically one can then calculate the transition rate constant  $k_{AB}$ . While feasible, this is an expensive procedure. It is more convenient to divide the calculation of  $C(t)$ , or, equivalently, of the free energy  $W_{AB}(t)$ , into two parts. In one part the free energy  $W_{AB}(t')$  is determined for a particular time  $t'$  (the time  $t'$  can be chosen small to make the simulation more efficient). In the second part of the calculation this free energy is complemented with the free energy to change the time at which the constraint to reach  $B$  is applied:

$$W_{AB}(t) = W_{AB}(t') + \Delta W_{AB}(t; t') . \quad (65)$$

The free energy  $\Delta W_{AB}(t, t')$  is the reversible work required to change the length of reactive trajectories and can be written in terms of the ratio of correlation functions,

$$\exp(-\Delta W_{AB}(t, t')) = \frac{C(t)}{C(t')} = \frac{\langle h_A(x_0)h_B(x_t) \rangle}{\langle h_A(x_0)h_B(x_{t'}) \rangle} . \quad (66)$$

This ratio can be computed efficiently for all times  $t, t' < \mathcal{T}$  from a single path sampling simulation [12]:

$$\exp(-\Delta W_{AB}(t, t')) = \frac{\langle h_B(x_t) \rangle_{AB}^*}{\langle h_B(x_{t'}) \rangle_{AB}^*} . \quad (67)$$

where the notation  $\langle h_B(x_t) \rangle_{AB}^*$  indicates an average over an ensemble of pathways starting in  $A$  but only required to visit  $B$  at some time slice along the path rather than ending in  $B$ . The correlation function  $C(t)$  then is

$$C(t) = \frac{\langle h_B(x_t) \rangle_{AB}^*}{\langle h_B(x_{t'}) \rangle_{AB}^*} \times C(t') \quad (68)$$

and the rate constant can be obtained from the plateau value of

$$k(t) \equiv \frac{dC(t)}{dt} = \frac{\langle \dot{h}_B(x_t) \rangle_{AB}^*}{\langle h_B(x_{t'}) \rangle_{AB}^*} \times C(t') , \quad (69)$$

where the dot indicates a time derivative. It is important to emphasize that the time correlation function  $C(t)$  is calculated exactly in the transition path sampling method and that no assumption about an underlying separation of time scales is made. Rather, the specific form of  $C(t)$  can reveal whether such a separation exists.

## 5.5 Transition Interface Sampling and Partial Path Sampling

Transition Interface Sampling (TIS) is a path sampling technique for the calculation of reaction rate constants [37, 38]. In this method, based on the determination of effective fluxes through hypersurfaces in phase space, the use of pathways with variable length and a reduced sensitivity to recrossing events leads to an enhanced efficiency with respect to the methods described in the previous sections. For diffusive dynamics a further efficiency increase can be achieved by using the partial path transition interface sampling (PPTIS) method [38, 39]. This approach is applicable to processes such as the nucleation of a phase transition or the folding of a protein, where due to strong coupling to the environment memory of prior motion is rapidly lost [20].

Central to the derivation of the rate constant expressions used in the TIS approach is the definition of *overall* states  $\mathcal{A}$  and  $\mathcal{B}$  denoted by calligraphic letters. A point  $x$  in phase space is defined to be part of the overall region  $\mathcal{A}$  of a trajectory started in  $x$  and followed backward in time reaches the product region  $A$  before the reactant region  $B$  (see Fig. 15). Thus the overall region  $\mathcal{A}$  contains all phase space points that lie directly in  $A$  plus all phase space points that, in a sense, originate from  $A$ . Similarly  $x$  is defined to be in  $\mathcal{B}$  if the respective backwards trajectory reaches  $B$  before  $A$ . Note that such overall

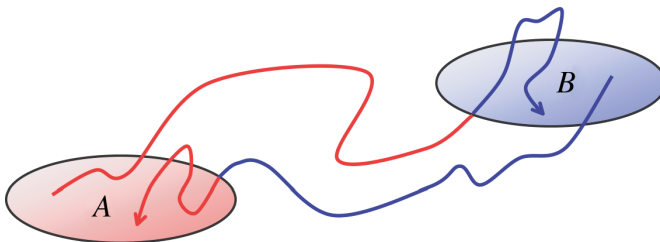


**Fig. 15.** Overall state  $\mathcal{A}$  is defined to consist of all phase space points  $x$  whose projections into configuration space either lie in the reactant region  $A$  and all points that reach region  $A$  before region  $B$  when propagated backward in time. Overall region  $\mathcal{B}$  is defined similarly. Hence, the trajectory segments colored in light gray belong to overall state  $\mathcal{A}$  while those colored in dark gray belong to  $\mathcal{B}$

states can be defined unambiguously only for deterministic dynamics. The overall states  $\mathcal{A}$  and  $\mathcal{B}$  cover the entire phase space and have a well defined, possibly highly fractal boundary between each other.

We can now use the characteristic functions  $h_{\mathcal{A}}(x)$  and  $h_{\mathcal{B}}(x)$  of the overall states to define the time correlation function,

$$\mathcal{C}(t) \equiv \frac{\langle h_{\mathcal{A}}(x_0)h_{\mathcal{B}}(x_t) \rangle}{\langle h_{\mathcal{A}} \rangle}. \quad (70)$$

This time correlation function is the conditional probability that a phase space point in  $\mathcal{A}$  at time 0 will be found in  $\mathcal{B}$  at time  $t$ . This correlation function for the overall states has the advantage that for regions  $A$  and  $B$  that are sufficiently far apart recrossings of the phase space hypersurface separating the overall states are essentially eliminated and the reaction rate constant  $k_{AB}$  can be identified with the slope of  $\mathcal{C}(t)$  at time 0:

$$k_{AB} = \frac{\langle h_{\mathcal{A}}(x_0)\dot{h}_{\mathcal{B}}(x_0) \rangle}{\langle h_{\mathcal{A}} \rangle} = \frac{\langle \phi_{AB} \rangle}{\langle h_{\mathcal{A}} \rangle}. \quad (71)$$

The second part of the equations defines the *effective positive flux*  $\langle \phi_{AB} \rangle$ , the average flux into region  $B$  stemming from trajectories coming directly from  $A$ . (Here, “directly” means that only the first entry of the trajectory into  $B$  is counted). This expression is equivalent to the transitions state theory (TST) rate constant for transitions from the overall state  $\mathcal{A}$  and  $\mathcal{B}$ . This approximation is valid in most cases due to the particular definition of the overall states in phase space. Since transitions from  $A$  to  $B$  (and hence also from  $\mathcal{A}$  to  $\mathcal{B}$ ) are rare, the TIS rate expression (71) cannot be evaluated by simple MD-simulation. Rather, a route similar to the umbrella sampling approach described in the previous paragraphs can be taken. For this purpose it is convenient to introduce a sequence of  $n$  non-intersecting dividing surfaces defined by  $\lambda(x) = \lambda_i$  (see Fig. 16). The order parameter  $\lambda(x)$  and the values  $\lambda_0, \lambda_1, \dots, \lambda_n$  are chosen such that the boundaries of regions  $A$  and  $B$  correspond to  $\lambda(x) = \lambda_0$  and  $\lambda(x) = \lambda_n$ , respectively. For each pair of surfaces  $i$  and  $j$  one then defines the crossing probability  $\mathcal{P}_A(j|i)$  as follows:

$\mathcal{P}_A(j|i)$  = Probability that a path crossing surface  $i$  for the first time after coming from region  $A$  reaches surface  $j$  before going back to  $A$ .

Using a concatenation of such transition probabilities for consecutive surfaces the TIS expression for the reaction rate constant can be rewritten as

$$k_{AB} = \frac{\langle \phi_{AB} \rangle}{\langle h_{\mathcal{A}} \rangle} = \frac{\langle \phi_{A1} \rangle}{\langle h_{\mathcal{A}} \rangle} \prod_{i=1}^{n-1} \mathcal{P}_A(i+1|i), \quad (72)$$

where  $\langle \phi_{A1} \rangle$  is the average flux through surface 1 stemming from trajectories coming directly from  $A$ . Note that the time dependence in (72) has become

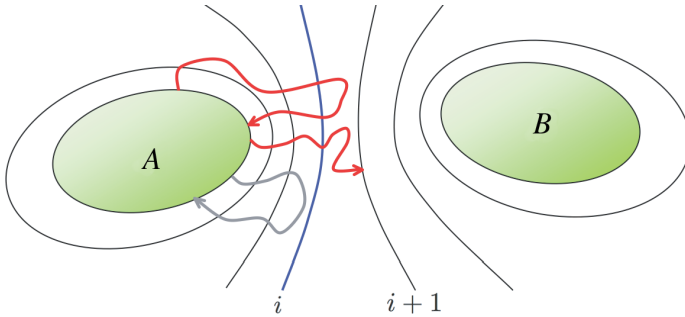


**Fig. 16.** In a transition interface sampling simulation to calculate the probability  $\mathcal{P}_A(i+1|i)$  the shooting algorithm is used to sample an ensemble of pathways that originate in  $A$ , cross interface  $i$  and then return to  $A$  or proceed to interface  $i+1$ . Then,  $\mathcal{P}_A(i+1|i)$  equals the fraction of the trajectories that reach interface  $i+1$  rather than the surface of  $A$ . The dark gray pathways depicted are members of this ensemble but the light gray one is not because it does not cross interface  $i$  before returning to  $A$

implicit. Instead of reaching a plateau in time as in (69), the factors appearing in (72) reach a plateau as a function of the order parameter.

In (72) the effective flux  $\langle \phi_{AB} \rangle$  is expressed as a product of the effective flux through surface 1,  $\langle \phi_{A1} \rangle$  and the probability that a trajectory that crosses interface 1 will reach  $B$  before  $A$  written as a product of crossing probabilities between consecutive interfaces. Each factor appearing in (72) can be determined easily with computer simulations. While the effective flux  $\langle \phi_{A1} \rangle$  can be computed from a straightforward MD simulation carried out in the reactant region  $A$ , the probabilities  $\mathcal{P}_A(i+1|i)$  can be calculated with path sampling simulations. More specifically, one defines an ensemble of pathways with variable length that are required to originate from  $A$ , cross surface  $i$  and then proceed to surface  $i+1$  or go back to  $A$ . This ensemble can be sampled with the shooting algorithm complemented with efficiency enhancing time reversal moves [38]. For strongly diffusive dynamics the calculation of the transition probabilities  $\mathcal{P}_A(i+1|i)$  can be simplified leading to a further efficiency increase. This approach, that views transitions as resulting from a sequence of uncorrelated hopping events is called partial path transition interface sampling (PPTIS) [39]. Note that the milestoning method proposed by Faradjan and Elber [40] and collaborators is very similar in spirit to PPTIS. Another method for the calculation of reaction rate constant that relies on the definition of a sequence of hypersurfaces and is based on (72) is the forward flux method of Allen, Warren, and ten Wolde [41].

## 5.6 Calculating Activation Energies with Transition Path Sampling

The temperature dependence of many rate constants for chemical reactions follows the Arrhenius law [42],  $k = \nu \exp(-\beta E_a)$ , where  $\nu$  is the so-called pre-exponential factor,  $E_a$  is the activation energy, and  $\beta = 1/k_B T$  is the inverse temperature. Both the activation energy  $E_a$  and the pre-exponential factor  $\nu$  can be determined from experimental data by plotting the logarithm of the reaction rate constant  $k$  as a function of  $\beta$ . While the negative slope of this line is the activation energy, the pre-exponential factor  $\nu$ , can be determined from the intersect of the  $\ln k$  vs.  $\beta$  curve with the  $y$ -axis. In the framework of transition state theory the activation energy  $E_a$  is the potential energy difference between reactants and the transition state, usually identified with a saddle point on the potential energy barrier separating reactants from products. The pre-exponential factor  $\nu$  depends on the entropy difference between reactants and transition state and it also includes dynamical corrections.

Since the Arrhenius parameters  $E_a$  and  $\nu$  are accessible experimentally, their theoretical prediction is of great interest. In principle, these parameters can be determined computationally by calculating the reaction rate constant as a function of temperature and then proceeding in a manner analogous to the analysis of the experimental data. The calculation of rate constants for reactions occurring in complex systems, however, is computationally expensive. For this reason, a direct calculation of kinetic observables, such as the activation energy, is highly desirable. This can be accomplished with a transition path sampling procedure [43]. This approach to determine activation energies does not require full rate constants calculations. Instead, the derivative of the reaction rate constant with respect to the inverse temperature  $\beta$  is expressed in terms of transition path averages which can be evaluated directly in a transition path sampling simulation. Since the transition path sampling method does not require any knowledge of mechanisms or transition states, this approach can be used to determine activation energies in complex systems where such knowledge is usually unavailable.

## 6 Rare Events in Trajectory Space

As a consequence of the second law of thermodynamics, the average work required to change an external parameter (for instance the position of a piston sliding in or out of a gas-filled cylinder) is larger than the Helmholtz free energy difference between the two equilibrium states corresponding to the initial and final value of the external parameter [34, 44]:

$$\langle W \rangle \geq \Delta F. \quad (73)$$

If the control parameter is changed reversibly, the average work  $\langle W \rangle$  is equal to the free energy difference  $\Delta F$ . (This is the reason that the term *reversible work* is often used for as a synonym of the equilibrium free energy difference.)

Remarkably, the so called Clausius inequality (73) can be changed into an equality by averaging the exponential  $\exp(-\beta W)$  instead of the work  $W$  [45, 46]:

$$\langle \exp(-\beta W) \rangle = \exp(-\beta \Delta F), \quad (74)$$

Here, the angular brackets  $\langle \dots \rangle$  denote an average over an ensemble of non-equilibrium transformations initiated from states distributed according to a canonical distribution. This relation, first proven by Jarzynski in 1997, relates equilibrium free energies to the statistics of work expended along non-equilibrium trajectories.

From a computational point of view the Jarzynski equality is interesting, because it permits the calculation of free energy differences from simulations in which a control parameter is switched at arbitrary speed. To be more specific, consider a system with Hamiltonian  $\mathcal{H}(x, \lambda)$  depending on the phase space point  $x$  and the control parameter  $\lambda$ . By changing  $\lambda$  continuously from its initial value  $\lambda_0$  to its final value  $\lambda_1$  the Hamiltonian  $\mathcal{H}(x, \lambda_0)$  of the initial state is transformed into that of the final state  $\mathcal{H}(x, \lambda_1)$ . The free energy difference

$$\Delta F = -k_B T \ln \frac{\int dx \exp\{-\beta \mathcal{H}(x, \lambda_1)\}}{\int dx \exp\{-\beta \mathcal{H}(x, \lambda_0)\}} = -k_B T \ln \frac{Q_1}{Q_0} \quad (75)$$

can be calculated by first generating initial conditions distributed according to  $\exp\{-\beta \mathcal{H}(x, \lambda_0)\}/Q_0$ . Then, the equations of motion of the system are integrated starting from these initial conditions. While the system evolves in time, the control parameter is switched from its initial to its final value. Along each trajectory the work necessary to switch the control parameter  $\lambda$  is determined and averaged according to (74).

The Jarzynski equality is exactly valid for arbitrary switching rates. This seems to suggest that free energy differences can be calculated in a computationally convenient way by averaging over short and therefore inexpensive trajectories. However, the statistical accuracy of the calculation rapidly degrades as the switching rate is increased [47–49]. The reason, familiar from applications of Zwanzig's exponential averaging approach [21, 50] or Widom's particle insertion method [51], is that exponential averages are dominated by rare but important work values. As the switching rate increases and the work distribution is shifted towards larger values, fewer and fewer trajectories contribute significantly to the exponential average causing large statistical fluctuations in the estimated free energy. These statistical difficulties can easily offset the gain originating from the low computational cost of short trajectories. For straightforward fast switching simulations this statistical problem limits the switching rates to values for which the average work does not deviate from the free energy difference by more than the thermal energy  $k_B T$  [48]. In this regime, however, fast switching simulations are not superior to conventional methods such as umbrella sampling and thermodynamic integration [48, 49].

A possible route to overcome the statistical problems occurring in a straightforward application of Jarzynski's equality was recently suggested by Sun [52].

The basic idea of Sun's approach is to favor the generation of those trajectories that mostly contribute to the exponential average by using a biased sampling scheme based on transition path sampling. This work biased sampling of fast switching trajectories was implemented by Sun in a thermodynamic integration framework [52], but it can easily be adapted to an umbrella sampling simulation in path space [49,53,54]. In all these approaches the transition path sampling methods discussed in the earlier sections of this article are used to select the rare trajectories with important work values. While first results have validated this approach [49, 52–54], further research is necessary to establish whether the combination of fast switching simulations with transition path sampling algorithms yields computational methods that are competitive with conventional approaches.

## Acknowledgments

This work was supported by the Austrian Science Foundation (FWF) under Grant No. P17178-N02. The authors are grateful to Jürgen Köfinger, Elisabeth Schöll-Paschinger, Harald Oberhofer, and Wolfgang Lechner for useful discussions.

## Appendix: Response to Large Perturbations

In this Appendix we justify the approach followed in Sect. 5 to derive microscopic expressions for the reaction rate constants. The standard way to do this for the reaction



occurring at low concentrations of species  $A$  and  $B$  is to relate the solution (48) of the phenomenological rate equations (46) with the relaxation of a non-equilibrium state prepared by applying an external perturbation. It can then be shown that in the case of weak perturbations (i.e., in the lineare response limit) the non-equilibrium relaxation has the same form as the autocorrelation of spontaneous population fluctuations:

$$\frac{\bar{N}_A(t) - \langle N_A \rangle}{\bar{N}_A(0) - \langle N_A \rangle} = \frac{\langle \delta h_A(0) \delta h_A(t) \rangle}{\langle (\delta h_A(0))^2 \rangle}, \quad (77)$$

where  $\delta h_A(x) = h_A(x) - \langle h_A \rangle$  and  $h_A(t) = h_A(x_t)$ . Here we show that for chemical reactions described by the rate equations (46) on a phenomenological level the assumption of a weak perturbation is unnecessary and that the same results can be obtained for perturbations of arbitrary strength. Consider a system with Hamiltonian  $\mathcal{H}_0(x)$  where  $x$  represents the coordinates and momenta of all particles in the system. The system contains  $N$  molecules that can exist either in state  $A$  or in state  $B$ . The characteristic functions  $h_A[q^{(i)}]$

and  $h_B[q^{(i)}]$  can be used to test whether molecule  $i$  is in state  $A$  or state  $B$ . Here,  $q^{(i)}$  denotes the coordinates of all atoms in molecule  $i$ . In equilibrium, the average number of molecules of type  $A$  and  $B$  is

$$\langle N_A \rangle = N \int dx \rho_0(x) h_A[q^{(i)}] \quad \text{and} \quad \langle N_B \rangle = N \int dx \rho_0(x) h_B[q^{(i)}], \quad (78)$$

where we have averaged over the equilibrium ensemble

$$\rho_0(x) = \frac{\exp(-\beta \mathcal{H}_0(x))}{\int dx \exp(-\beta \mathcal{H}_0(x))}. \quad (79)$$

Now imagine that a perturbation

$$\Delta \mathcal{H}(x) = -\varepsilon \sum_i^N h_A[q^{(i)}] \quad (80)$$

is coupled to the system and the system is allowed to equilibrate at temperature  $T$  under the action of the new Hamiltonian

$$\mathcal{H}(x) = \mathcal{H}_0(x) + \Delta \mathcal{H}(x) \quad (81)$$

leading to the new equilibrium distribution

$$\rho(x) = \frac{\exp(-\beta[\mathcal{H}_0(x) + \Delta \mathcal{H}(x)])}{\int dx \exp(-\beta[\mathcal{H}_0(x) + \Delta \mathcal{H}(x)])}. \quad (82)$$

For positive values of the perturbation strength  $\varepsilon$  the species  $A$  is favored with respect to species  $B$  in the new equilibrium state. If the perturbation is removed the number of molecules of type  $A$  relaxes back to its equilibrium value  $\langle N_A \rangle$ . The average number  $\overline{N}_A(t)$  of molecules of type  $A$  present in the system at a time  $t$  after the perturbation is switched off is given by the non-equilibrium average

$$\overline{N}_A(t) = \frac{\int dx \exp(-\beta[\mathcal{H}_0(x) + \Delta \mathcal{H}(x)]) \sum_i^N h_A[q_t^{(i)}]}{\int dx \exp(-\beta[\mathcal{H}_0(x) + \Delta \mathcal{H}(x)])}, \quad (83)$$

where  $q_t^{(i)}$  is the configuration of molecule  $i$  at time  $t$  and the time evolution of the system after the perturbation is removed is governed by the unperturbed Hamiltonian  $\mathcal{H}_0(x)$ . For the specific perturbation from (80) the nonequilibrium average is

$$\overline{N}_A(t) = \frac{\int dx \exp(-\beta \mathcal{H}_0(x)) \exp(\beta \varepsilon \sum_i^N h_A[q^{(i)}]) \sum_i^N h_A[q_t^{(i)}]}{\int dx \exp(-\beta \mathcal{H}_0(x)) \exp(\beta \varepsilon \sum_i^N h_A[q^{(i)}])}. \quad (84)$$

In the conventional treatment of unimolecular kinetics [34, 55] one evaluates this average in the limit of weak perturbation strength  $\varepsilon$  by expanding the

above expression in a Taylor series. Truncating the series after the term linear in  $\varepsilon$  yields the well known linear response result:

$$\bar{N}_A(t) - \langle N_A \rangle = N\beta\varepsilon \langle \delta h_A(0)\delta h_A(t) \rangle. \quad (85)$$

Hence, the response to a weak perturbation is completely determined by the equilibrium fluctuations of the system. From the above equation an expression for the reaction rate constant can be derived [34].

The assumption of weak perturbations, however, is unnecessary and the nonequilibrium average can be evaluated exactly for arbitrary perturbation strengths. To do that we first divide both numerator and denominator on the right hand side of (84) by  $\int dx \exp(-\beta\mathcal{H}_0(x))$  obtaining:

$$\bar{N}_A(t) = \frac{\langle \exp(\beta\varepsilon \sum_i^N h_A[q^{(i)}]) \sum_i^N h_A[q_t^{(i)}] \rangle}{\langle \exp(\beta\varepsilon \sum_i^N h_A[q^{(i)}]) \rangle}. \quad (86)$$

The Boltzmann factor in the above equation originating from the perturbation can be written as a product:

$$\exp\left(\beta\varepsilon \sum_i^N h_A[q^{(i)}]\right) = \prod_i^N \exp(\beta\varepsilon h_A[q^{(i)}]) = \prod_i^N f_A[q^{(i)}, \varepsilon], \quad (87)$$

where, to simplify the notation, we have introduced the function  $f_A[q^{(i)}, \varepsilon] \equiv \exp(\beta\varepsilon h_A[q^{(i)}])$ .

The nonequilibrium average thus becomes:

$$\bar{N}_A(t) = \frac{\sum_i^N \langle \prod_j^N f_A[q^{(j)}, \varepsilon] h_A[q_t^{(i)}] \rangle}{\langle \prod_j^N f_A[q^{(j)}, \varepsilon] \rangle}. \quad (88)$$

Since the solution is assumed to be sufficiently dilute such that all molecules are statistically independent from each other the numerator and the denominator in the above equation can be written as

$$\begin{aligned} \sum_i^N \left\langle \prod_j^N f_A[q^{(j)}, \varepsilon] h_A[q_t^{(i)}] \right\rangle &= \sum_i^N \left( \langle f_A[q^{(i)}, \varepsilon] h_A[q_t^{(i)}] \rangle \prod_{j \neq i} \langle f_A[q^{(j)}, \varepsilon] \rangle \right) \\ &= \left( \sum_i^N \frac{\langle f_A[q^{(i)}, \varepsilon] h_A[q_t^{(i)}] \rangle}{\langle f_A[q^{(i)}, \varepsilon] \rangle} \right) \prod_j^N \langle f_A[q^{(j)}, \varepsilon] \rangle \end{aligned} \quad (89)$$

and

$$\left\langle \prod_j^N f_A[q^{(j)}, \varepsilon] \right\rangle = \prod_j^N \langle f_A[q^{(j)}, \varepsilon] \rangle, \quad (90)$$

respectively. Inserting these two expressions into (88) we obtain

$$\bar{N}_A(t) = \sum_i^N \frac{\langle f_A[q^{(i)}, \varepsilon] h_A[q_t^{(i)}] \rangle}{\langle f_A[q^{(i)}, \varepsilon] \rangle} = N \frac{\langle f_A[q, \varepsilon] h_A[q_t] \rangle}{\langle f_A[q, \varepsilon] \rangle}, \quad (91)$$

where we have omitted the superscripts in the last part of the equation because all of the  $N$  molecules are equivalent.

Now, the function  $f_A[q, \varepsilon]$  can take only two different values depending on whether the corresponding molecule is in state  $A$  or not:

$$f_A[q, \varepsilon] = \exp(\beta \varepsilon h_A[q]) = \begin{cases} \exp(\beta \varepsilon) & \text{if } q \in A, \\ 1 & \text{if } q \notin A. \end{cases} \quad (92)$$

Therefore, we can write  $f_A[q, \varepsilon]$  in terms of the characteristic function  $h_A$ :

$$f_A[q, \varepsilon] = \exp(\beta \varepsilon h_A[q]) = h_A[q](e^{\beta \varepsilon} - 1) + 1. \quad (93)$$

Using this expression we obtain

$$\begin{aligned} \bar{N}_A(t) &= N \frac{\langle \{(e^{\beta \varepsilon} - 1)h_A(q) + 1\} h_A(q_t) \rangle}{\langle (e^{\beta \varepsilon} - 1)h_A(q) + 1 \rangle} \\ &= N \frac{(e^{\beta \varepsilon} - 1)\langle h_A(q)h_A(q_t) \rangle + \langle h_A \rangle}{(e^{\beta \varepsilon} - 1)\langle h_A \rangle + 1}. \end{aligned} \quad (94)$$

Thus, an initial excess  $\bar{N}_A(0)$  of species  $A$  decays to its equilibrium value  $\langle N_A \rangle$  according to:

$$\bar{N}_A(t) - \langle N_A \rangle = N(e^{\beta \varepsilon} - 1) \frac{\langle \delta h_A(q) \delta h_A(q_t) \rangle}{(e^{\beta \varepsilon} - 1)\langle h_A \rangle + 1}. \quad (95)$$

where we have used that  $\langle N_A \rangle = N\langle h_A \rangle$ . This results implies that the response of the system to a perturbation of arbitrary strength is completely determined by its equilibrium fluctuations. Nevertheless, the response to the perturbation is a nonlinear function of the perturbation strength  $\varepsilon$ . Expansion of the above expression into a power series in  $\beta \varepsilon$  and truncation after the linear term yields the familiar linear response expression of (85).

The standard linear response derivation [34] of expressions for the reaction rate constants rests on the observation that the *relative* deviation from the equilibrium average generated by a weak perturbation decays in the same way as the equilibrium fluctuations normalized by their initial value:

$$\frac{\bar{N}_A(t) - \langle N_A \rangle}{\bar{N}_A(0) - \langle N_A \rangle} = \frac{\langle \delta h_A(q) \delta h_A(q_t) \rangle}{\langle [\delta h_A(q)]^2 \rangle}. \quad (96)$$

It is thus sufficient that the relaxation of the nonequilibrium population is *proportional* to the decay of equilibrium fluctuations. While the above expression (also known as Onsager's regression hypothesis) follows for weak perturbations, a linear dependence of the system's response on the perturbation

strength  $\varepsilon$  it is not necessary. In fact, the exact expressions (95) derived above for perturbations of arbitrary strength also leads to the behavior described by (96). Hence, for the type of chemical dynamics considered here, Onsager's regression hypothesis remains exactly valid also for the relaxation of arbitrarily large excess populations. This result justifies the approach used in Sect. 5 (we started with all molecules of type *A*) to derive expressions for the reaction rate constant.

## References

1. H.-X. Zhou and R. Zwanzig (1991) A rate process with an entropy barrier. *J. Chem. Phys.*, **94**, pp. 6147–6152
2. J. B. Anderson (1973) Statistical theories of chemical reactions: Distributions in the transition region. *J. Chem. Phys.*, **58**, pp. 4684–4692; C.H. Bennett (1977) Molecular Dynamics and Transition State Theory: the Simulation of Infrequent Events. In *Algorithms for Chemical Computations*, ed. R. E. Christoffersen, pp. 63–97; Washington, D.C.: Amer. Chem. Soc.; D. Chandler (1978) Statistical mechanics of isomerization dynamics in liquids and the transition state approximation. *J. Chem. Phys.*, **68**, pp. 2959–2970
3. L.R. Pratt (1986) A statistical method for identifying transition states in high dimensional problems. *J. Chem. Phys.*, **85**, pp. 5045–5048
4. C. Dellago, P.G. Bolhuis, F.S. Csajka, and D. Chandler (1998) Transition Path Sampling and the Calculation of Rate Constants. *J. Chem. Phys.*, **108**, pp. 1964–1977
5. C. Dellago, P.G. Bolhuis, and D. Chandler (1998) Efficient Transition Path Sampling: Applications to Lennard-Jones cluster rearrangements. *J. Chem. Phys.*, **108**, pp. 9236–9245
6. P.G. Bolhuis, C. Dellago, and D. Chandler (1998) Sampling ensembles of deterministic transition pathways. *Faraday Discuss.*, **110**, pp. 421–436
7. W. E, W. Ren, and E. Vanden-Eijnden (2002) String method for the study of rare events. *Phys. Rev. B*, **66**, 052301/1–4
8. W. E, W. Ren, and E. Vanden-Eijnden (2005) Finite Temperature String Method for the Study of Rare Events. *J. Phys. Chem. B*, **109**, pp. 6688–6693
9. R. Elber, A. Ghosh, A. Cardenas, and H. Stern (2004) Bridging the gap between reaction pathways, long time dynamics and calculation of rates. *Adv. Chem. Phys.*, **126**, pp. 93–129
10. D. Passerone, M. Ceccarelli, and M. Parrinello (2003) A concerted variational strategy for investigating rare events. *J. Chem. Phys.*, **118**, pp. 2025–2032
11. P. G. Bolhuis, D. Chandler, C. Dellago, and P.L. Geissler (2002) Transition Path Sampling: Throwing Ropes over Mountain Passes in the Dark. *Ann. Rev. Phys. Chem.*, **53**, pp. 291–318
12. C. Dellago, P.G. Bolhuis, and P.L. Geissler (2002) Transition Path Sampling. *Adv. Chem. Phys.*, **123**, pp. 1–78
13. C. Dellago and D. Chandler (2002) Bridging the time scale gap with transition path sampling, in *Molecular Simulation for the Next Decade*, ed. by P. Nielaba, M. Mareschal, and G. Ciccotti, Springer, Berlin. pp. 321–333
14. C. Dellago (2005) Transition Path Sampling, in *Handbook of Materials Modeling*, ed. by S. Yip, Springer, Berlin. pp. 1585–1596

15. C. Dellago (2006) Transition Path Sampling and the Calculation of Free Energies, in *Free energy calculations: Theory and applications in chemistry and biology*, ed. by A. Pohorille and C. Chipot, Springer, Berlin, pp. 265–294
16. G.E. Crooks and D. Chandler (2001) Efficient transition path sampling for non-equilibrium stochastic dynamics. *Phys. Rev. E*, **E 64**, 026109/1–4
17. R. Car and M. Parrinello (1985) Unified Approach for Molecular Dynamics and Density-Functional Theory. *Phys. Rev. Lett.*, **55**, pp. 2471–2474
18. S. Nose (1984) A unified formulation of the constant temperature molecular dynamics methods. *J. Chem. Phys.*, **81**, pp. 511–519; W.G. Hoover (1985) Canonical dynamics: Equilibrium phase-space distributions”, *Phys. Rev. A*, **31**, pp. 1695–1697
19. D.J. Evans, W.G. Hoover, B.H. Failor, B. Moran, and A.J.C. Ladd (1983) Non-equilibrium molecular dynamics via Gauss’s principle of least constraint. *Phys. Rev. A*, **28**, pp. 1016–2021
20. R. Zwanzig (2001) *Nonequilibrium Statistical Mechanics*, Oxford University Press, Oxford
21. M.P. Allen and D.J. Tildesley (1987) *Computer Simulation of Liquids*, Clarendon Press, Oxford
22. S. Chandrasekhar (1943) Stochastic Problems in Physics and Astronomy. *Rev. Mod. Phys.*, **15**, pp. 1–89
23. P.L. Geissler, C. Dellago, D. Chandler, J. Hutter, and M. Parrinello (2001) Autoionization in liquid water. *Science*, **291**, pp. 2121–2124
24. D.P. Landau and K. Binder (2000) *A Guide to Monte Carlo Simulations in Statistical Physics*, Cambridge University Press, Cambridge
25. N. Metropolis, A.W. Rosenbluth, M.N. Rosenbluth, A.H. Teller, and E. Teller (1953) Equation of State Calculations by Fast Computing Machines. *J. Chem. Phys.*, **21**, pp. 1087–1092
26. T.J.H. Vlugt, C. Dellago, and B. Smit (2000) Diffusion of Isobutane in Silicalite studied by Transition Path Sampling. *J. Chem. Phys.*, **113**, p. 8791
27. P.G. de Gennes (1971) Reptation of a Polymer Chain in the Presence of Fixed Obstacles. *J. Chem. Phys.*, **55**, pp. 572–579
28. R.B. Best and G. Hummer (2005) Reaction coordinates and rates from transition paths. *Proc. Nat. Acad. Sci. USA*, **102**, pp. 6732–6737
29. L. Onsager (1938) Initial Recombination of Ions. *Phys. Rev.*, **54**, pp. 554–557
30. V. Pande, A.Y. Grosberg, T. Tanaka, and E.I. Shakhnovich (1998) On the transition coordinate for protein folding. *J. Chem. Phys.*, **108**, pp. 334–350
31. S. Auer and D. Frenkel (2001) Prediction of absolute crystal-nucleation rate in hard-sphere colloids. *Nature*, **409**, pp. 1020–1023
32. E.A. Carter, G. Ciccotti, J.T. Hynes, and R. Kapral (1989) Constrained reaction coordinate dynamics for the simulation of rare events. *Chem. Phys. Lett.*, **156**, pp. 472–477
33. D. Moroni, P.R. ten Wolde, and P.G. Bolhuis (2005) Interplay between Structure and Size in a Critical Crystal Nucleus. *Phys. Rev. Lett.*, **94**, 235703/1–4
34. D. Chandler (1987) *Introduction to Modern Statistical Mechanics*, Oxford University Press, New York
35. G.M. Torrie and J.P. Valleau (1974) Monte Carlo free energy estimates using non-Boltzmann sampling: Application to the sub-critical Lennard-Jones fluid. *Chem. Phys. Lett.*, **28**, pp. 578–581
36. C. Dellago, P.G. Bolhuis and D. Chandler (1999) On the calculation of rate constants in the transition path ensemble. *J. Chem. Phys.*, **110**, pp. 6617–6625

37. T.S. van Erp, D. Moroni, and P.G. Bolhuis (2003) A novel path sampling method for the calculation of rate constants. *J. Chem. Phys.*, **118**, pp. 7762–7774
38. T.S. van Erp and P.G. Bolhuis (2005) Elaborating transition interface sampling methods. *J. Comp. Phys.*, **205**, pp. 157–181
39. D. Moroni, P.G. Bolhuis, and T.S. van Erp (2004) Rate constants for diffusive processes by partial path sampling. *J. Chem. Phys.*, **120**, pp. 4055–4065
40. A.K. Faradjian and R. Elber (2004) Computing time scales from reaction coordinates by milestoneing. *J. Chem. Phys.*, **120**, pp. 10880–10889
41. R. J. Allen, P. B. Warren, and P. R. ten Wolde (2005) Sampling Rare Switching Events in Biochemical Networks. *Phys. Rev. Lett.*, **94**, 018104/1–4
42. P.W. Atkins (2001) *Physical Chemistry, 7th edition*, Oxford University Press, Oxford
43. C. Dellago and P.G. Bolhuis (2004) Activation energies from transition path sampling simulations. *Mol. Sim.*, **30**, pp. 795–799
44. H.B. Callen (1985) *Thermodynamics and an Introduction to Thermostatistics, 2nd edition*, John Wiley and Sons, New York
45. C. Jarzynski (1997) Nonequilibrium Equality for Free Energy Differences. *Phys. Rev. Lett.*, **78**, pp. 2690–2693
46. G.E. Crooks (1998) Nonequilibrium Measurements of Free Energy Differences for Microscopically Reversible Markovian Systems. *J. Stat. Phys.*, **90**, pp. 1481–1487
47. F. Ritort (2003) Work fluctuations and transient violations of the second law: perspectives in theory and experiments. *Sem. Poincare* **2**, pp. 193–226
48. G. Hummer (2001) Fast-growth thermodynamic integration: Error and efficiency analysis. *J. Chem. Phys.*, **114**, pp. 7330–7337
49. H. Oberhofer, C. Dellago and P.L. Geissler (2005) Biased sampling of non-equilibrium trajectories: Can fast switching simulations outperform conventional free energy calculation methods? *J. Phys. Chem. B*, **69**, pp. 6902–6915
50. R. Zwanzig (1954) High-Temperature Equation of State by a Perturbation Method. I. Nonpolar Gases. *J. Chem. Phys.*, **22**, pp. 1420–1426
51. B. Widom (1963) Some Topics in the Theory of Fluids. *J. Chem. Phys.*, **39**, pp. 2808–2812
52. S.X. Sun (2003) Equilibrium free energies from path sampling of nonequilibrium trajectories. *J. Chem. Phys.*, **118**, pp. 5769–5775
53. F.M. Ytreberg and D.M. Zuckerman (2004) Single-ensemble nonequilibrium path-sampling estimates of free energy differences. *J. Chem. Phys.*, **120**, pp. 10876–10879
54. M. Athènes (2004) A path-sampling scheme for computing thermodynamic properties of a many-body system in a generalized ensemble. *Eur. Phys. J. B*, **38**, pp. 651–663
55. D. Frenkel and B. Smit (2002) *Understanding Molecular Simulation*, Academic Press, San Diego